KfK 4084
September 1987

Evaluation of the Urania Equation of State Based on Recent Vapour Pressure Measurements

E. A. Fischer
Institut für Neutronenphysik und Reaktortechnik
Projekt Schneller Brüter

Kernforschungszentrum Karlsruhe

KERNFORSCHUNGSZENTRUM KARLSRUHE
Institut für Neutronenphysik und Reaktortechnik

Projekt Schneller Brüter

KfK 4084

EVALUATION OF THE URANIA EQUATION OF STATE BASED ON RECENT VAPOUR PRESSURE MEASUREMENTS

E.A. Fischer

Kernforschungszentrum Karlsruhe GmbH, Karlsruhe

Kernforschungszentrum Karlsruhe GmbH
Postfach 3640, 7500 Karlsruhe 1

ISSN 0303-4003

Abstract

In the past few years, new experimental results on the vapour pressure of UO_2 up to extremely high temperatures became available. These vapour pressure data, obtained by advanced experimental techniques, are lower than the ones used so far at KfK. It was, therefore, appropriate to carry out a complete new evaluation of the equation of state (EOS) of UO_2. The Significant Structures Theory by Eyring, which was extended to the case of non-stoichiometric urania, was applied for this work. The extended theory is described in some detail. By a suitable choice of the model parameters, good agreement of the evaluated EOS with recent experimental data was obtained, which is additional evidence for the reliability and consistency of the recent data. The extrapolation predicts a critical temperature of 10600 K, which is higher than earlier predictions. Analytical fits for the important state variables were produced for convenient use in fast reactor accident analysis codes.

Neuauswertung der Zustandsgleichung für UO_2 unter Benutzung neuerer Dampfdruckmessungen

Zusammenfassung

In den letzten Jahren wurden neue experimentelle Daten für den Dampfdruck über UO_2 bis zu extrem hohen Temperaturen verfügbar. Diese Dampfdruckdaten, die mit weiter entwickelten experimentellen Techniken produziert wurden, liegen niedriger als die bisher bei KfK verwendeten. Dies war der Anlaß für eine Neuauswertung der Zustandsgleichung für UO_2. Für die Auswertung wurde die "Significant Structures Theory" von Eyring verwendet, die für nicht-stoichiometrisches Uranoxid erweitert wurde. Die erweiterte Theorie wird hier beschrieben. Durch geeignete Wahl der Modellparameter gelang es, gute Übereinstimmung mit den experimentellen Daten zu erreichen. Dies ist ein zusätzlicher Hinweis auf die Zuverlässigkeit und Konsistenz der neueren Daten.

Das Modell führt auf eine kritische Temperatur von 10600 K, die höher liegt als die bisherigen Extrapolationen. Es wurden analytische Anpassungen für die wichtigsten Zustandsgrößen produziert, die in einfacher Weise in den Codes für Reaktor-Störfall-Analysen verwendet werden können.

Table of Contents

1. Introduction

The analysis of hypothetical core disruptive accidents (e.g. loss-of-flow accident with failure to scram) plays an important role in the assessment of fast reactor safety. Though such accidents are expected to be non-energetic, certain accident paths which lead to power excursions with significant energy release cannot be ruled out. To estimate the energy produced in the fuel during an excursion, and the subsequent conversion of thermal to mechanical energy in the post-disassembly expansion phase, the pressure buildup in the fuel must be known.

If fission product pressure is absent, or is neglected in the analysis, it is usually the fuel vapour pressure which acts as a shut down mechanism of the excursion. In such energetic accident paths, the fuel temperature is predicted to increase up to typically 5000 K, and the fuel is in a two-phase state. Thus, the fuel vapour pressure curve is certainly a key state variable, which must definitely be known for accident studies. However, other state variables are also needed; e.g. the liquid density to study cases where single-phase liquid pressures are responsible for the shut down, or the liquid entropy for analysing the conversion of thermal to work energy during the post-disassembly expansion phase. Therefore, knowledge of the vapour pressure curve is not sufficient; rather, one needs the complete equation of state (EOS) for a systematic and consistent accident analysis, including the excursion and the expansion phase. Though the critical temperature is generally not reached in accident analysis calculations, the position of the critical point is so important for determining the different regions of the p-V-T diagram that its prediction is a key point in EOS analysis. It should be noted that apart from the applications to reactor work, there is also scientific interest in a complete and thermodynamically consistent EOS for UO_2.

The fuel EOS which has been used so far at KfK in the accident analysis codes SAS, SIMMER, and KADIS is based essentially on an extrapolation of early vapour pressure measurements over UO_2, which was carried out by Menzies /1/ in 1966. At that time, experimental vapour pressure data were available only over solid UO_2, so that a large extrapolation was needed, which necessarily introduced significant uncertainties. In addition, it was tacitly assumed that the EOS of UO_2 can also be used for the fast reactor (U, Pu) mixed oxide fuel.

Since then, advanced experimental techniques were developed to dynamically heat fuel samples above the melting point for vapour pressure measurements, either by laser surface heating, or by in-pile fission heating. Both techniques have their specific problems, which will not be discussed here. Consequently, the early published results have rather large errors. In the past few years, however, both techniques were developed to rather high standards, and indeed could be used to produce reliable vapour pressure data at temperatures far above the melting point. The more recent data are all consistent, and indicate that the vapour pressure used in the earlier EOS is too high. Therefore, a new EOS evaluation for UO_2 was carried out using the following important new experimental data:

- In-pile vapour pressure measurements over UO_2 and mixed oxide by Breitung and Reil /2/ were completed and reported in 1985. The in-pile technique has the advantage that both the time scale (a few ms) and mode of heating by nuclear fission are typical of the reactor case. In a considerable effort towards developing this technique to a high standard, the authors succeeded in overcoming the main problems. Large flux depressions and fuel motion, which would introduce uncertainties in the energy input, could be avoided, making use of the excellent pulsing capabilities of the ACRR reactor. In these experiments, extremely high temperatures, up to about 8000 K, were reached.
- Vapour pressure measurements over liquid UO_2 by Bober et al /3/ using a boiling point method, and laser surface heating of the sample, were completed in 1985. The samples were

heated in a pressure cell in an inert gas atmoshpere. This method avoids the main problem of earlier laser heating experiments with evaporation into vacuum, namely the correlation of the measured evaporation rate with the equilibrium vapour pressure.

- Ohse et al /4/ investigated, in 1985, the enhanced emission of charged particles, an effect which is typical of the evaporation into vacuum in laser surface heating experiments. By considering this effect in the evaluation of measured data, the authors obtained an improved equilibrium vapour pressure curve.
- Limon et al /5/ used the boiling point technique in 1981 for in-pile measurements of the UO_2 vapour pressure in the SILENE reactor. An important weak point in these experiments, which are clearly not truly recent experiments, is the non-negligible flux depression within the sample. It is, however, believed that the error due to this effect is within reasonable limits /2/.
- In addition, measurements of the liquid density with good accuracy were carried out by Drotning (1981) /6/. The results agree with earlier experiments (1963) by Christensen /7/. The data can be used now with much more confidence because two independent experiments gave consistent results, while before 1981 only one single experiment was available.
- The vapour pressure over solid UO_2 was determined with good accuracy by Ackermann et al /8/ in 1979. These authors carried out a re-assessment of all the available experimental data, and recommended an "international average" vapour pressure over UO_2 at the reference temperature 2150 K. This work provided a reference base point with which all the extrapolations should be consistent.

The classical theoretical models which were applied in earlier evaluations of the UO_2 EOS, including prediction of the critical point, are the principle of corresponding states /1/, and the Significant Structures Theory (SST) /9, 10/. Both models are based on strongly simplifying assumptions. More recently, the perturbed hard core model was also applied for UO_2 /11/.

The major shortcoming of these methods is the assumption of single-component evaporation, i.e. liquid stoichiometric UO_2 evaporates into gaseous UO_2. In reality, the U-O system contains different species in the vapour phase, namely UO_3, UO, and oxygen. Their ratios depend on the oxygen-to-metal ratio of the liquid fuel.

Therefore, it is desirable to include these different vapour species in the EOS evaluation. Out of the available models, the SST lends itself most easily to such an extension. Therefore, this extended SST was selected for the present work.

With this model, the EOS data for non-stoichiometric $UO_{2\pm x}$ can be obtained. In principle, it would be feasible to further extend the model for (U, Pu) mixed oxide. It is, however, not planned to carry out such an extension, firstly because Breitung and Reil /2/ did not see a significant difference in vapour pressure between UO_2 and mixed oxide. Secondly, thermodynamic data for PuO_2 are much more scarce than for UO_2, so that an evaluation for mixed oxide would introduce additional open parameters. These parameters would have to be fitted to the same vapour pressure measurements, and therefore such an extension would not provide any additional information. It is, therefore, recommended to use the new UO_2 EOS also for the fast reactor mixed oxide fuel.

2. Theoretical Approach

The theoretical approaches used so far to evaluate the UO_2 EOS up to the critical point are the principle of corresponding states /1/, the significant structures theory (SST) /9, 10/, and more recently, the perturbed hard core model (PHC) /11/. The PHC theory has a much more secure theoretical foundation than the older models. On the other hand, SST and PHC gave very similar results. This is illustrated by comparing the critical point data in the following table.

Critical Point Data of UO_2 Obtained by SST and PHC

(based on older experimental data)

	T_c(K)	p_c(Mpa)	V_c(m^3/mol)	Z_c
SST (1976) /10/	7560	122.0	163×10^{-6}	0.32
PHC (1985) /11/	7567	140.9	156×10^{-6}	0.35

As the difference of about 15 % in the pressure can be considered as minor, this comparison provides a verification of the (older) SST method against the more recent PHC, which is on firmer theoretical grounds.

Indeed, the results seem to depend much more on the input data, than on the model. However, one shortcoming common to all these approaches is the assumption that the vapour phase consists only of UO_2 gas. In reality, UO_3, UO and atomic oxygen give equally important contributions to the vapour pressure.

This shortcoming is avoided in the extrapolations of the vapour pressure by Green and Leibowitz /12/ and by Long et al. /13/. Both are based essentially on the law of mass action. However, neither of these extrapolations produces a complete set of EOS data. The approach described in this paper is an extension of the SST model to non-stoichiometric UO_2, which avoids both the shortcomings discussed above. The SST is a statistical mechanical model where the partition function of the liquid is obtained by combining the partition functions of the solid and of the gas. In the extension, an oxygen defect model is introduced into the solid partition function. This model includes oxygen vacancies and interstitials; their concentration depends on the oxygen chemical potential μ_o. Similarly. the species UO and UO_3 are included in the gas phase; their ratio depends again on μ_o. This is a system, which in statistical mechanics, is described by a grand partition function. The model will be described in detail in the following Section. The SST was chosen for this work because it lends itself rather easily to this necessary extension. A concise account of this work was presented recently at the BNES Conf. on Science and Technology of Fast Reactor Safety /14/.

3. Equations of the Extended Significant Structures Theory

In this Section, the assumptions of the extended theory will be established and the equations developed. First, it is shown how the thermodynamics of the non-stoichiometric system $UO_{2\pm x}$, with its multicomponent vaporization, can be described by a Grand Partition Function. Then, introducing the Significant Structure Theory, one finds that it is necessary to extend both the "solidlike" and the "gaslike" partition function to the non-stoichiometric case. An oxygen point defect model is chosen for the"solidlike" case, while the "gaslike" partition function is extended to the case of a multicomponent gas phase.

3.1 The Grand Partition Function for $UO_{2\pm x}$

In statistical mechanics, the usual canonical partition function (PF) for one mol of a single-component substance in a given volume V, at temperature T, is defined by

$$Z(T,V) = \int d\varepsilon \omega(\varepsilon) d^{-\varepsilon/kT} \tag{1}$$

where $\omega(\varepsilon)$ is the density of energy levels, which depends on V. Z is connected with the Helmholtz free energy F(T,V) in the following way

$$F(T,V) = -kT \ln Z \tag{2}$$

Equation(2) relates the statistical mechanics quantity Z to thermodynamic state variables. From the thermodynamic relation

$$dF = -SdT - pdV$$

one finds that S and p are obtained as derivatives of the Helmholtz free energy. All the other state variables are combinations of such derivatives.

The canonical PF is applicable only for a single-component substance. For a thermodynamic description of non-stoichiometric $UO_{2\pm x}$, with its multicomponent evaporation, we want to develop a formalism based on a grand partition function (GPF), which is also a well-known tool in statistical mechanics. First, one has to consider the dependence of Z on the number of oxygen atoms per mol of $UO_{2\pm x}$, N_o, so that $Z = Z(T,V,N_o)$. Clearly, $N_o/N = 2\pm x$ This number is usually different in the liquid and in the vapour, and is determined, in each phase, by the chemical potential of atomic oxygen, μ_o. For liquid and vapour in equilibrium, one has the condition

$$\mu_o^{liq} = \mu_o^{gas}$$

Such a system can be described by a GPF, which is defined as

$$GPF(T,V,\mu_o) = \sum_{N_o} \exp\left(\frac{\mu_o N_o}{kT}\right) Z(T,V,N_o) \tag{3}$$

Strictly speaking, (3) is a semi-GPF, rather than a GPF, because the sum is only over N_o, whereas the number of uranium atoms is fixed, corresponding to one mol. However, for simplicity , the term GPF will be retained.
The thermodynamic potential corresponding to (3) is /15/

$$J(T,V,\mu_o) = -kT \ln(GPF) \tag{4}$$

It is equal to

$$J = U - TS - \mu_o N_o$$

and the differential of J is

$$dJ = -SdT - pdV - \bar{N}_o d\mu_o$$

From this equation, one finds that the state variables, S,p, and $\bar{N}_o$, the average of N_o over the grand canonical ensemble , are obtained from the derivatives

$$S = -\left(\frac{\partial J}{\partial T}\right)_{V,\mu_o} \qquad p = -\left(\frac{\partial J}{\partial V}\right)_{T,\mu_o} \qquad \bar{N}_o = -\left(\frac{\partial J}{\partial \mu_o}\right)_{T,V} \tag{5}$$

We follow the notation by Becker /15/; note that a somewhat different one is used in other textbooks, e.g. Fowler and Guggenheim /16/. According to the second eq.(5), the pressure is given by the slope of the J versus V curve at constant T and μ_o. On the co-existence curve, the pressure in the liquid and the vapour phase must be equal, i.e.

$$\left(\frac{\partial J}{\partial V}\right)_{V_l} = \left(\frac{\partial J}{\partial V}\right)_{V_g}$$

Thus, the well-known double tangent method /10,17/ can be used to obtain the specific volumes of the two phases, and the vapour pressure, for given T and μ_o. Note that $\bar{N}_o$ is different in the liquid and in the gas, as it should. However, as the critical temperature is approached, the two volumes become equal, and therefore also the $\bar{N}_o$ values.
We now introduce the concept of the Significant Structures Theory (SST), which is described in detail e.g. in /10,17/. The basic assumption is that the PF of the liquid is composed of a solid-like part f_s, and a gaslike part, f_g:

$$\ln Z(T,V) = N \frac{V_s}{V} \ln f_s(T,V) + N \frac{V - V_s}{V} \ln f_g(T,V) \tag{6}$$

where V_s is the specific volume of the solid $UO_{2\pm x}$ at the melting point, and N is Avogadro's number.

The solidlike part is the same as in earlier work /10/ except that the "excess enthalpy" term in f_s is omitted. Thus, one has

$$\begin{aligned} \ln f_s = {} & \frac{E_s}{RT} \left(\frac{V}{V_s}\right)^{\gamma} - 9 \ln(1 - \exp(-\Theta_E/T)) \\ & + 3 \ln\left[1 + n\left(\frac{V}{V_s} - 1\right) \exp\left(- \frac{a E_s V_s}{3 RT(V - V_s)} \left(\frac{V}{V_s}\right)^{\gamma}\right)\right] \end{aligned} \tag{7}$$

where
- E_s binding energy of the UO_2 crystal
- Θ_E Einstein temperature of the UO_2 crystal
- R gas constant
- a,n,γ model parameters.

The gaslike part is composed of translational, rotational, vibrational and electronic excitation contributions

$$f_g = Q^{trans}\, Q^{rot}\, Q^{vib}\, Q^{el} \tag{8}$$

The equations (6-8), which are the same as in /10/, are essentially those proposed originally by Eyring /17/. They will not be discussed in detail, as their properties were studied extensively in the literature, see e.g. /17/ and the references given in /10/.
Note, however, that these equations hold for stoichiometric UO_2, which (fictitiously) evaporates into the single component UO_2 (gas). For the present work, it is necessary to extend both f_s and f_g to include the dependence on N_o. For the solid PF, the extension will be carried out using a simple oxygen defect model; for the gas PF, by including the species UO and UO_3. Thus,

$$\ln f_s(T,V) \longrightarrow \ln f_s(T,V) + \ln Z_{def}(T,N_o) \tag{9}$$

$$\ln f_g(T,V) \longrightarrow \ln f_g(T,V) + \ln Z_{gm}(T,N_o) \tag{10}$$

In the following it is more convenient to use the number of "non-stoichiometric" oxygen atoms, $N_b = N_o - 2N$, rather than N_o, assuming that the reference state for lnZ is the stoichiometric state. One can now introduce the eqns. (9) and (10) into the GPF, and obtains

$$\mathrm{GPF}\,(T,V,\mu_o) = f_s(T,V)^{N\frac{V_s}{V}}\; f_g(T,V)^{N\frac{V-V_s}{V}} \sum_{N_b} \exp\Big[N\frac{V_s}{V}\Big(\frac{\mu_o N_b}{kT} + \ln Z_{def}(T,N_b)\Big) + N\,\frac{V-V_s}{V}\Big(\frac{\mu_o N_b}{kT} + \ln Z_{gm}(T,N_b)\Big)\Big] \tag{11}$$

The GPF, as defined by this equation, is the key function of the method used in this paper. It includes terms for solid-like and gaslike urania, with different O/M, but it does not explicitly contain a term for oxygen. The chemical potential μ_o is equivalent to defining an oxygen partial pressure, with which the liquid and gaseous urania phases are in equilibrium. Thus, it determines the O/M of both phases.

3.2 The Non-Stoichiometric Part of the Grand Partition Function

3.2.1 The Defect Partition Function

To account for non-stoichiometry in the solidlike PF, it is necessary to introduce a suitable oxygen potential model.
In this paper, a defect model was chosen, which includes oxygen vacancies, and interstitial oxygen atoms in the solidlike lattice. A simple model of this kind was proposed by Thorn and Winslow /18/ in 1966. Although, more advanced models, usually with more complex types of defect, were developed since /19-21/, the simple Thorn-Winslow formalism is used in this paper. The idea is to keep the model simple, mainly because the SST is a highly simplified model on its own, and it would not be meaningful to combine it with a complex defect model. Besides, there is no general agreement as to which of the more recent models can be considered most reliable. It should be mentioned, that a very recent oxygen potential model, proposed by Hyland /21/, is again of the simple type.
The PF for the oxygen vacancies and interstitials is given by

$$\text{Defect PF} = \sum_{N_v, N_i} \frac{(2N)!}{N_v!\,(2N - N_v)!} \; \frac{N!}{N_i!\,(N - N_i)!} \; q_v(T)^{N_v} \, q_i(T)^{N_i} \exp\left(\frac{N_i(\varepsilon_i + \mu_o) - N_v(\varepsilon_v + \mu_o)}{kT}\right) \tag{12}$$

where N_i, N_v are the numbers of interstitials and vacancies per mol /18/; $\varepsilon_i, \varepsilon_v$ are the energies to remove an interstitial, or a lattice atom to infinity. The functions q_i and q_v account for the vibrational modes associated with the defects.
According to Thorn and Winslow we have /18/

$$\ln q_v(T) = -3\left[\frac{\theta_v}{2T} + \ln(1 - e^{-\theta_v/T})\right] - \text{Const}$$

$$\ln q_i(T) = -3\left[\frac{\theta_i}{2T} + \ln(1 - e^{-\theta_i/T})\right] \tag{13}$$

We now observe that $N_b = N_i - N_v$, and each term in (12) contains the factor $\exp(N_b\mu_o/kT)$. We want to write (12) as a sum over N_b and N_v.
Alternatively, one could also retain N_i as independent quantity but we choose N_v. This leads to an expression of the form

$$\text{Defect PF} = \sum_{N_b} \exp\left(\frac{\mu_o N_b}{kT}\right) \sum_{N_v} \Phi(N_b + N_v, N_v, kT) \tag{14}$$

where, for simplicity, ϕ is not written down explicitly.
When this expression is compared with eq. (11), it is obvious that Z_{def}, as introduced in (11), must be identified as follows

$$Z_{def}(T, N_b)^N = \sum_{N_v} \Phi(N_b + N_v, N_v, kT) \tag{15}$$

This equation shows that Z_{def} includes the summation over N_v, but not over N_b.

To find a simpler expression for Z_{def}, we first replace the factorials in eq.(12) as follows

$$N! = \left(\frac{N}{e}\right)^N \tag{16}$$

This approximation is standard in statistical mechanics. Furthermore, statistical mechanics /15/ tells that a sum such as that over N_v is practically equal to the maximum term of the sum,

$$\sum_{N_v} \Phi \approx \Phi(\text{max.term}) = \Phi(N_b + N_v^m, N_v^m, kT)$$

where N_v^m, the most probable value of N_v, is determined by the condition

$$\frac{\partial \Phi(N_b + N_v, N_v, kT)}{\partial N_v} = 0$$

In the following, we will simply write N_v instead of N_v^m for the number which gives the maximum term.
In addition, we introduce the variables

$$\Theta_v = \frac{N_v}{2N} \qquad\qquad x = \frac{N_b}{N} \tag{17}$$

where X is positive for the hyperstoichiometric and negative for the substoichiometric material. With these simplifications, one obtains in a straightforward manner

$$\begin{aligned} \ln Z_{def}(T,x) = 2 \Big[&-\theta_v \ln\theta_v - (1-\theta_v)\ln(1-\theta_v) \\ &- \theta_v(\ln q_v + \frac{\varepsilon_v}{kT})\Big] - (x+2\theta_v)\ln(x+2\theta_v) - (1-x-2\theta_v) \\ &\ln(1-x-2\theta_v) + (x+2\theta_v)(\ln q_i + \frac{\varepsilon_i}{kT}) \end{aligned} \tag{18}$$

The value of θ_v to be used in this equation is the one that maximizes the expression on the right hand side; it is determined by

$$\frac{\partial}{\partial \theta_v} \ln Z_{def}(T,\mathbf{x},\theta_v) = 0 \tag{19}$$

where $\ln Z_{def}(T,x,\theta_v)$ is simply the right hand side, regarded as a function of θ_v. Note that the variable x has replaced N_b.
The condition (19) can be written in an explicit form

$$\frac{\theta_v(x - 2\theta_v)}{(1 - \theta_v)(1 - x - 2\theta_v)} = A = \frac{q_i}{q_v} \exp\left(\frac{\varepsilon_i - \varepsilon_v}{kT}\right) \tag{20}$$

The solution for θ_v is

$$\theta_v = \frac{1}{4(1 - A)} \left[-(x + (3 - x)A) + \sqrt{(x + (3 - x)A)^2 + 8A(1 - A)(1 - x)} \right]$$

3.2.2 The Non-Stoichiometric Part of the Gas Partition Function

The vapour phase in equilibrium with liquid $UO_{2\pm x}$ consists of several species. The more important uranium bearing species, which are included in the present model, are UO, UO_2, and UO_3. Gaseous U has such a low concentration that it can be neglected. The pressure of ions (e.g. UO_2^+, UO_3^- /22/) is also neglected. After deciding to include three species, it is a straight-forward matter to develop the GPF for one mol of vapour, assuming again that the oxygen chemical potential μ_o is given.

Let Z_i be the (macroscopic) PF for N_i particles of UO_i. It is given by

$$Z_i = \frac{(f_i V)^{N_i}}{N_i!}$$

where f_i , the PF for one molecule, is of the form

$$\ln f_i = \frac{n}{2} \ln T - \sum \ln (1 - e^{-\theta_v/T}) + \ln Q^{el} \tag{21}$$

$$+ K_i - 1 + \ln N_i$$

In this equation, the θ_v belong to the vibrational frequencies, Q^{el} is the electronic PF, K_i is a constant (see Appendix B). The canonical PF of a mixture containing N_1, N_2, N_3 particles of UO, UO_2, UO_3 is then

$$Z_{gas} = \frac{(f_1 V)^{N_1}}{N_1!} \frac{(f_2 V)^{N_2}}{N_2!} \frac{(f_3 V)^{N_3}}{N_3!} \tag{22}$$

If instead the chemical potentials of the species, μ_1, μ_2, μ_3, are given, one obtains the GPF as a sum over the particle numbers

$$GPF_{gas} = \sum_{N_1,N_2,N_3} \exp\left(\frac{N_1\mu_1 + N_2\mu_2 + N_3\mu_3}{kT}\right) Z_{gas}(T,V,N_1,N_2,N_3) \tag{23}$$

The following relations hold in equilibrium

$$\mu_1 + \mu_o = \mu_2 \qquad\qquad \mu_2 + \mu_o = \mu_3 \tag{24}$$

where μ_i is the chemical potential of UO_i.

Using these relations, one can write the GPF

$$GPF_{gas} = \sum_{N_1,N_3} \exp\left(\frac{N\mu_2 + (N_3 - N_1)\mu_o}{kT}\right) Z_{gas}(T,V,N_1,N-N_1-N_3,N_3) \tag{25}$$

The equilibrium ratios of the N_i follow from the relations (24)

$$\frac{N_1}{N_2} = \frac{f_1}{f_2}\, e^{-\mu_o/kT} \qquad\qquad \frac{N_3}{N_2} = \frac{f_3}{f_2}\, e^{+\mu_o/kT} \tag{26}$$

However, this implies that the partition functions Z_i are normalized to the same energy level at T = 0, i.e.

$$f_i \longrightarrow f_i \exp\left(\frac{\Delta H_i}{RT}\right)$$

where ΔH_i is the enthalpy of formation of UO_i ($i \neq 2$) from UO_2 and oxygen at T = O.

We now assume that we have one mol of vapour, so that N is fixed, rather than μ_2. The factor $\exp(N\mu_2/kT)$ and the sum over N must then be dropped. Observing that $N_b = N_3 - N_1$, we obtain the final form of the gas GPF

$$GPF_{gas} = \left(\frac{f_2 eV}{N}\right)^N \sum_{N_b} \exp\left(\frac{N_b \mu_o}{kT}\right) \sum_{N_1} \left(\frac{N}{N - 2N_1 - N_b}\right)^{N-2N_1-N_b} \left(\frac{N}{N_1}\right)^{N_1} \left(\frac{N}{N_b + N_1}\right)^{N_b+N_1} \left(\frac{f_1}{f_2}\right)^{N_1} \left(\frac{f_3}{f_2}\right)^{N_b+N_1} \tag{27}$$

The logarithm of GPF_{gas} can now be written

$$\ln GPF_{gas} = N \ln \frac{f_2 eV}{N} + \ln\left[\sum_{N_b} \exp\left(\frac{N_b \mu_o}{kT}\right) \sum_{N_1} \phi_{gas}(N_b+N_1, N_1, kT)\right] \tag{28}$$

where again ϕ_{gas} is introduced as an abbreviation; the full expression can be easily obtained from (27). A comparison of this equation (28) with (11) shows that the first term (for UO_2) is just the stoichiometric part of the PF for the gaslike molecules. The non-stoichiometric part ("gas mixture") $Z_{gm}(T,N_b)$ is then defined by the relation

$$\left[Z_{gm}(T,N_b)\right]^N = \sum_{N_1} \phi_{gas}(N_b+N_1, N_1, kT) \tag{29}$$

where Z_{gm} is a sum over N_1 (number of UO atoms in one mol of gas mixture), but not over N_b.

A simple expression can again be obtained for Z_{gm}, in the same way as for the defect PF, applying the following steps

- Approximate the factorials as in eq.(16)
- Replace the sum over N_1 by its maximum term
- Introduce the variables $y_1 = N_1/N$ and $x = N_b/N$

This procedure leads to

$$\ln Z_{gm}(T,x) = y_1(\ln \frac{f_1}{f_2} - \ln y_1) + (x + y_1)(\ln \frac{f_3}{f_2} - \ln(x + y_1)) \qquad (30)$$

$$- (1 - x - 2y_1)\ln(1 - x - 2y_1)$$

The value of y_1 is determined by the "maximum" condition

$$\frac{\partial}{\partial y_1} \ln Z_{gm}(T,x,y_1) = 0 \qquad (31)$$

This condition is a quadratic equation for y_1

$$\frac{y_1(x + 2y_1)}{(1 - x - 2y_1)^2} = \frac{f_1 f_3}{f_2^2} = a \qquad (32)$$

with the explicit solution

$$y_1 = \frac{1}{2(1 - 4a)} \left[- x - 4a(1 - x) + \sqrt{x^2(1 - 4a) + 4a} \right]$$

3.2.3 The Non-Stoichiometric Partition Function

We are now in a position to specify how to calculate the non-stoichiometric part of the GPF. Going back to eq.(11), we first observe that also the sum over N_b can be replaced by the maximum term. If the expression in the square bracket, or rather 1/N times this expression, is designated $\phi + \mu_o x/kT$, we have

$$\phi(T,V,x,\theta_v,y_1) + \frac{\mu_o x}{kT} = \frac{V_s}{V} \ln Z_{def}(T,x,\theta_v) + \frac{V - V_s}{V} \ln Z_{gm}(T,x,y_1) + \frac{\mu_o x}{kT} \tag{33}$$

where $\ln Z_{def}$ and $\ln Z_{gm}$ are given by (18) and (30). ϕ depends explicity on the three variables x, θ_v, y_1, which must be determined by the three following conditions:

Condition 1 : $\frac{\partial \phi}{\partial x} + \frac{\mu_o}{kT} = 0$

By taking the derivatives of the equations (18) and (30), one obtains

$$\frac{V_s}{V}\left[- \ln \frac{x + \theta_v}{1 - x - 2\theta_v} + \ln q_i + \frac{\varepsilon_i}{kT}\right] + \frac{V - V_s}{V}\left[- \ln \frac{x + y_1}{1 - x - 2y_1} + \ln \frac{f_3}{f_2}\right] + \frac{\mu_o}{kT} = 0 \tag{34}$$

Condition 2: $\frac{\partial \phi}{\partial \theta_v} = 0$

As the variable θ_v occurs only in $\ln Z_{def}$, this condition is simply the eq.(20)

Condition 3: $\frac{\partial \phi}{\partial y_1} = 0$

This condition is expressed by the eq.(32).

While conditions 2 and 3 are explicit equations, eq.(34) which states the condition 1 cannot be solved explicitly for x. Therefore, a suitable (iterative) numerical method must be used to find x as a function of V and μ_o.
It is known that for both the hyperstoichiometric and for the important part of substoichiometric range, x is larger in the gas phase than in the condensed phase. In a first approximation, assuming that y_1 and $2\theta_v$ are not too much different, this means that the condition

$$\ln \frac{f_3}{f_2} > \ln q_i + \frac{\varepsilon_i}{kT} \qquad (35)$$

must hold. This condition is well fullfilled at the melting point if reasonable data are used. However, when choosing data suitable for extrapolation, one has to make sure that eq.(35) is fullfilled up to the critical temperature.
At this point, the construction of the Grand Partition Function is completed, and therefore the theory is completely defined. The state variables, internal energy U, pressure and their derivatives, can then be obtained by differentiation of the GPF. The basic equations are given in Appendix A. However, it is not trivial to obtain the equations for the non-stoichiometric contributions to the state variables because of the above conditions. Therefore, the appropriate equations are also listed in Appendix A.

3.2.4 Additional Comments

It is obvious that the Clausius-Clapeyron equation does not hold in its simple form for a multicomponent system, but it can be extended to this case as follows (at constant μ_o)

$$\left(\frac{dp_{sat}}{dT}\right)_{\mu_o} = \frac{Q - \mu_o(x_g - x_l)}{T(V_g - V_l)} \tag{36}$$

Q is the difference in the average enthalpy between the equilibrium gas mixture and the liquid.
Also, from straightforward thermodynamics

$$\left(\frac{dp_{sat}}{d\mu_o}\right)_T = \frac{x_g - x_l}{V_g - V_l} \tag{37}$$

In the cases of interest, there is usually $x_g > x_l$. Then, an increase in the oxygen chemical potential leads to an increase in pressure (via increasing UO_3 density). Note that (36) and (37) are thermodynamic relations, which are independent of Eyring's model. The oxygen chemical potential μ_o determines the pressure of atomic oxygen, p_O, through the equation

$$RT \ln p_o = \mu_o + T(FEF)_o - (H^o_{298} - H^o_o)$$

where FEF is the free energy function of atomic oxygen. It is tabulated e.g. by Stull and Sinke /23/, up to 3000K. For a monatomic gas, the data can be safely extrapolated to higher temperatures, assuming $C_p = 5/2R$. At the temperatures of interest, the pressure p_{o2} of molecular oxygen is always a lot lower than p_o, and can be neglected in first approximation. Therefore, no values for the oxygen potential will be quoted in this paper. If desired, it can be estimated from the relation

$$\ln p_{o2} = 2 \ln p_o + \frac{2\Delta G_f^o(O)}{RT} \qquad (38)$$

where $\Delta G_f(O) = 256.803 - 67.564 \times 10^{-3} T$ (kJ/mol), from the JANAF Table /24/.
However, one should be aware that an extrapolation of a linear fit is valid only over a limited temperature range.

4. Selection of the Input Data

The selection of the model parameters was guided by the following considerations: As far as the parameters have a direct physical meaning, and measured data are available, they are used in the model. Second, the reference data should reproduce the recent (and reliable) experimental data discussed in the introduction.

4.1 Partition Functions for the Fuel Vapour Species

The thermodynamic functions of the fuel vapour species can, in principle, be calculated from spectroscopic data on the internal molecular degrees of freedom. This method is considered more reliable than just a linear extrapolation of the standard free energy of formation. In this work, the Born-Oppenheimer approximation is used, which allows to separate the PF into the following contributions

$$f_{gas} = Q^{trans}\, Q^{rot}\, Q^{vib}\, Q^{el}$$

The detailed equations used are given in Appendix B. The first three contributions can be readily calculated if the necessary spectroscopic data are available. The data are gathered in Table I. However, calculation of the electronic PF is more difficult.

For actinide oxides, the number of low-lying electronic levels is very large. Experimental data on the levels are not available, and a theoretical treatment, e.g. by a self-consistent field calculation, is very involved, and probably not possible with the required accuracy. Therefore, one has to use certain model assumptions, which clearly again puts limits on the accuracy of the results.

There are two principal ways to arrive at a PF for an actinide oxide /25/. One observes that, although no experimental data are available for oxides, data do exist for certain metal atoms and ions. Low lying electronic levels e.g. of UO must be those of the U^{2+} ion. This ion is isoelectronic with the Th atom, and should, therefore, have similar electronic states as Th. This is the basis of the Atomic States Model /26/: One calculates the PF for a reference metal atom (or ion) from the known experimental levels and uses it as an estimate for the oxide. This method yields a direct numerical estimate, though the accuracy is, of course, limited. It is believed that the Atomic States Model tends to overestimate the electronic PF. This method was used e.g. for U^{2+} (in UO), which is isoelectronic with Th, and for U^{4+} (in UO_2) isoelectronic with Th^{2+} /27/.
The general expression for the electronic PF is

$$Q^{el} = \sum_n g_n \exp(-\frac{\varepsilon_n}{kT}) \qquad (39)$$

where ε_n are the levels, g_n their multiplicities.
All the other models /25/ assume that the ε_n (and g_n) can be approximated as analytic functions, with certain parameters which still have to be determined. Here, we shall discuss only the method used in this paper. As the levels are rather dense, one can approximate the PF by an integral over the level density, and write it as follows

$$Q^{el} = g_o + \int_{E_1}^{E_i} D(E)\ \exp(-\frac{E}{kT})\, dE \qquad (40)$$

In our earlier work /10/, the level density was assumed constant. In addition, it was observed that the ionisation energy E_i is so large that the integral can be taken to infinity. In the present work, the model was slightly modified by allowing for a linear increase of the level density with energy, i.e.

$$D(E) = D_o + D_1 E \tag{41}$$

The electronic PF is then

$$Q^{el} = g_o + \int_{E_1}^{\infty} dE(D_o + D_1 E)\exp(-\frac{E}{kT})$$

As was mentioned before, the presently available molecule data base does not allow a reliable calculation of the electronic PF of the UO_2 molecule. Indeed, the uncertainty in the electronic PF is the main source of error in the vapour pressure extrapolation, and it seems resonable to work backward and adjust the assumed electronic level density so as to reproduce the experimental vapour pressure, provided the latter is sufficiently accurate and reliable /10, 25/. A prominent example of such a procedure is an extrapolation carried out by the equation-of-state group at Los Alamos National Laboratories /28/. A very high density of states (which was obtained by a relativistic self-consistent field calculation) was used to reproduce high experimental vapour pressures. Serious doubts were, however, expressed in the literature /13/ that this procedure might not be correct. It will turn out in the present work that the recent experimental vapour pressure data are consistent with "normal" electronic level density. By "normal" we mean that the level densities are comparable to those obtained from the Atom States Model. This finding settles the issue whether the very high level densities proposed by the Los Alamos Group should be used to calculate thermodynamic functions.

Ackermann et al. /1/ produced a "best vapour pressure equation" for UO_2 in the temperature range 1800 to 2600K. Thus, the vapour pressure is well established in this range, and since UO_2(gas) is the dominant species, this vapour pressure equation can be used to adjust the electronic PF of UO_2(gas).

According to the Third Law, the vapour pressure is determined by the free energy function (FEF) of the gas and the solid

$$R \ln p(\mathrm{at}) = (\mathrm{FEF})_{\mathrm{gas}} - (\mathrm{FEF})_{\mathrm{sol}} - \frac{\Delta H_{\mathrm{sub}}(298)}{T} \qquad (42)$$

In eq. (42), the value 618.4 kJ/mol (147.8 kcal/mol) for the heat of sublimation, ΔH_{sub}, was used /8/ because it is consistent with the vapour pressure curve. The $(\mathrm{FEF})_{sol}$ was taken from an earlier evaluation /10/. It differs from the data of the ANL evaluation /12/ only within the uncertainty range of 1 %. It was found that the vapour pressure curve in /1/ could be reproduced either (assuming D = const.) by

$$Q^{el} = 3 + \int_{25104}^{\infty} dE\; 5.76 \times 10^{-4} \exp\left(-\frac{E}{RT}\right) \qquad (43)$$

or, assuming a slight linear increase in D(E), by

$$Q^{el} = 3 + \int_{22593}^{\infty} dE\,(3.167 \times 10^{-4} + 4.54 \times 10^{-9} E) \exp\left(-\frac{E}{RT}\right) \qquad (44)$$

where E is in J/mol, and the gas constant is R = 8.314 J/molK.

It might be of interest to note that $\ln Q^{el}$ is numerically in the range 2 to 4, and contributes typically $\leq$ 5% to $\ln f_{gas}$. Though, this is only a small fraction , the vapour pressure is, according to eq. (42), rather sensitive to changes in $\ln Q^{el}$ because

$$\delta \ln p = \delta \ln Q^{el}$$

The fact, that the analysis of the vapour pressure curve leads to an electronic PF of the expected magnitude (comparable to Atomic States Model) indicates a high degree of consistency between the different data.

Table II shows a comparison of different evaluations of the FEF. Below the melting temperature, our data agree well with the ANL evaluation by Green. This is not surprizing because both evaluations were guided by the Ackermann et al. /8/ vapour pressure. Above the melting temperature, our PF increases slightly faster. It is, however, still below the results by Chasanov /27/, who used the Atomic States Model, observing that Th^{2+} is isoelectronic with U^{4+}. Note that there is little difference between the two equations (43) and eq.(44). However, the latter gives a slightly better fit to experimental data. The difference in UO_2 (gas) pressure at 6000K is only about 15%.
Uncertainties of data for UO and UO_3 are much larger than for UO_2. Green /25/ found that there are inconsistencies between the FEF obtained from spectroscopic data, and the thermodynamic data like free energy of formation. Besides the electronic PF, the reaction enthalpies ΔH_1 and ΔH_3 for the fictitious reactions

$$UO + O = UO_2 \qquad\qquad UO_2 + O = UO_3$$

at 0 K are needed.
The evaluation was again guided primarily by the requirement to obtain good agreement with the new experimental data. Furthermore, the partial pressures should be broadly consistent with experimental values obtained by mass spectrometry at the European Institute for Transuranium Elements (TU) /4/.The main quantity for comparison is the following ratio, see eq.(26)

$$\frac{N_1 N_3}{N_2^2} = \frac{f_1 f_3}{f_2^2}$$

or rather the square root of it. This ratio is independent of the oxygen potential , and the comparison is also valid if the effective O/M of the samples at high temperatures is not well known.

The congruent evaporating composition at the melting point is not well known. However, for a meaningful evaluation, one should certainly have $(O/M)_{con} \leq 1.94$. This poses a limit on the partial pressure of UO.

Some FEF values of UO are listed in Table III, Table VI shows the parameters of the electronic PF. The present evaluation is well consistent with the results of the Atomic States Model. In the latter, the levels of Th were used to construct the PF. However, the value ΔH_1 = -756.0 kJ/mol is somewhat more negative than the value -732.6 kJ/mol, which is derived from Green's evaluation /12/.

The FEF of UO_3, as shown in Table IV, needs some comments. For the present evaluation, we have ΔH_3 = 512.1 kJ/mol, as compared to 578.0 kJ/mol from the ANL data /12/. The electronic PF parameters are shown in Table VI. The U^{6+} ion is isoelectronic with Rn for which no low-lying electronic levels exist. Therefore, the ANL data by Green, and the earlier one by Chasanov were both obtained by assuming that there is no electronic contribution to the PF. With this assumption, which is clearly not well established, we were unable to reproduce the measured total vapour pressure, and also to obtain consistancy with the partial pressures measured by Ohse et al. /4/. Therefore, an electronic PF was constructed, which makes the FEF of UO_3 larger than the one of the ANL evaluation. On the other hand, our ΔH_3 is lower than that of ANL. The partial pressures obtained with these data are compared in Table V with those measured by Ohse et al. /4/, and with the ANL data. The Table shows that the partial pressures at the melting point are low, and comparable to the ANL values. This is desirable because experience tells that UO_2 (gas) is the dominant species well below the melting point. On the other hand, the contribution of the partial pressures of UO and UO_3 increases with temperature, which is consistent with the experimental values. Note that according to Ref./4/ the UO_3 partial pressure was measured only in the range 4000-4500K. Data outside this range were obtained by extrapolation.

4.2 Model Parameters

As was mentioned earlier, the oxygen potential, in this work, is described by a defect model, with the formalism suggested by Thorn and Winslow /18/. The data were adjusted essentially to Blackburn's model /19/. The oxygen potential at 3150K, as calculated from various oxygen potential models, are shown in Table VII.The first five lines of the table are taken from Ref./12/, Table 3. They show that there is large scatter, which corresponds to two orders of magnitude in the oxygen pressure. The evaluation by Green and Leibowitz favors a high value, whereas Hyland in his recent evaluation /21/, after examining the available experimental data carefully, recommends an oxygen potential which is close to ours. It is interesting to examine the extrapolated data at high temperature. The ANL evaluation gives at 6000K, an O_2 pressure of 11 MPa, plus an atomic oxygen pressure of 21 MPa, in equilibrium with $UO_{2.0}$. The sum of these two contributions is about three times larger than the experimental value obtained by Breitung and Reil /2/, or extrapolated from the Bober et al. /3/ data. Thus, these recent experimental results call for a lower oxygen potential, at least at high temperature, but it seems reasonable to use a lower value than Green and Leibowitz, also at the melting temperature.

The experimentally observed strong increase in the specific heat capacity of solid UO_2 above ~ 80% of the melting temperature has been the subject of extensive discussions and speculations in the literature /13, 29, 30/. It can be caused either by Frenkel defects, or by electronic disorder, or, more likely, by a combination of these two effects. It is not clear how this anomaly should be extrapolated into the liquid temperature range. Without going into any discussion in this paper, a rather ad hoc approach will be taken: It was found that eq.(7) for an Einstein crystal gives satisfactory results; especially, the experimental specific heat capacity c_p of liquid UO_2 is well reproduced by the model. This is indication that the "excess enthalpy" does not play a role in liquid UO_2, and therefore, no attempt was made to simulate it in this model.

The SST model involves several parameters (E_s, Θ_E, n, γ, a), which were determined by Eyring from basic considerations for simple liquids /17/. For the UO_2 molecule, these parameters must be adjusted to reproduce thermodynamic data which are known from experiment.

First, the triple point (assumed to be at 3120K) is defined by the condition that there are three values of J(V), corresponding to the solid, liquid, and gas volume, on a straight line. This line is also the double tangent at the liquid and the gas volume. Second, the liquid specific volume at the triple point is given by experiment, V_l = 30.87 cm^3/mol. These two conditions can be fulfilled by adjusting the parameters a and γ in eq.(7). Third, an effective Einstein temperature to be used in eq.(7) is found from the condition that the partial pressure of UO_2 (gas) for stoichiometric UO_2 (liq.) at 3120K, which was obtained by extrapolating the Ackermann et al. /8/ data to the triple point should be reproduced. The extrapolated value depends slightly on the gas partition function used. Fourth, the binding energy E_s of the model is adjusted to obtain a consistent slope of the vapour pressure at the triple point. This means that the heat of evaporation, H_g-H_l, is consistent with the slope of the UO_2 (gas) partial pressure. The selected parameters which satisfy these condition are shown in Table VIII.

4.3 Calculational Method

For a given temperature (below the critical temperature T_c), the double tangent on the curve $J(T,V,\mu)$ plotted as a function of V, is obtained by an iterative procedure. It defines the liquid and the vapor volumes V_l and V_g. For a given value of x and an estimate for V_l, μ_o is directly obtained from eq.(34). The value V_g and the corresponding value x_g for the saturated vapour are then obtained by iteration. In the next step, better values for V_l, μ_o and V_g are obtained, until the "outer" iteration has converged.

5. Discussion of the Results

5.1 Comparison with Experiments

As explained in section 4, it was the goal of the present work to obtain agreement of the evaluated EOS with recent experimental data. The following comparisons show that this goal could be reached remarkably well. Specifically, there is very good agreement with vapour pressure data obtained by different experimental techniques covering the wide temperature range from 2150 K to about 8000 K. The agreement is equally good for the vapour pressure versus enthalpy and the vapour pressure versus temperature measurements. These results provide additional evidence for the consistency between the different more recent experimental data. Moreover, they indicate that the present model, inspite of its limitations, is adequate for describing the EOS of a material as complicated as the urania phase.

In the following, the evaluated EOS will be compared in more detail with the experimental data. The SST vapour pressure versus specific enthalpy curve for stoichiometric UO_2 is shown in Fig. 1, together with the representative experimental data. The Breitung and Reil experiments were used as a guideline in the evaluation, and the selected curve is indeed in good agreement with these experimental data over the entire range of the measurements. This result is not trivial in view of the fact that the partial pressure of atomic oxygen increases much faster with increasing enthalpy than the pressure of the uranium-bearing species. At the lower end of the measurements, p(o) is only a few percent of the total pressure, while at the upper end it increases to about 30 %. The evaluated curve is not identical, but very close to the numerical fit presented by Breitung /2/; it reproduces the experimental data well also at the highest enthalpy. The fact that its slope also agrees with experiment indicates the extrapolation to even higher temperatures is reasonable. In addition, our curve is consistent within reasonable uncertainties with the experiments by Limon et al. /5/.

Fig. 2 shows the vapour pressure versus (inverse) temperature curve, together with the measurements. The temperature range (up to ~4800 K) is covered by the laser experiment data. Agreement with the experiments by Bober et al. /3/ and by Ohse et al. /4/ is remarkably good. The evaluated curve is also well consistent with the ANL data /31/, which are the only "low temperature" data that extend above the melting temperature. The deviation of the Limon et al. /5/ data is most likely due to experimental uncertainty, possibly the neutron flux depression in the sample. The new vapour pressure curve is lower than the curve by Menzies /1/, which was so far used in the accident analysis codes. E.g. at 5000 K, we have now 2.47 Mpa, as compared to 4.7 Mpa in the Menzies evaluation, and 6.3 Mpa in the recommendation by IAEA /36/. However, there is no doubt that the lower value is more reliable.

Consistency was also obtained with the liquid density measurements by Drotning /6/, (Fig. 3). These latter experiments cover a range of only a few hundred degrees in the liquid state, and it seems doubtful, at first sight, whether there is any justification in extrapolating them up to 10 000 K. However, the slope of the liquid density $\rho_l(T)$, seems to be well established in the vicinity of the melting point because the two available experiments by Drotning and by Christensen /7/ are in good agreement. Furthermore, one can argue that the only physical reason for the liquid density function $\rho_l(T)$ to deviate from a straight line is due to the approach to the critical temperature, and must be negative. This kind of behaviour was imposed as a condition on the evaluation. Note that as $\rho_l(T)$ decreases, the vapour density, and thus also the vapour pressure must increase, according to the law of rectilinear diameter. Thus, there is a thermodynamic relation between the two quantities, namely liquid density and vapour pressure (i.e. only the pressure of the U-bearing species, excluding the oxygen pressure), and it is gratifying that the present evaluation is consistent with measurements of both these quantities.

5.2 Vapour Pressure for Different O/M

The partial pressures were calculated as functions of temperature for different O/M values. Some important results are given in the Tables IX-XVII. These tables cover mainly the slightly sub-stoichiometric range, $1.90 \leq O/M \leq 2.00$, which is important for reactor fuel.

Note that the sensitivity of the total pressure to the condensed-phase O/M is large only near the melting point, where its magnitude is low. At higher temperatures, it depends only weakly on the O/M. The $UO_2(g)$ partial pressure is almost independent of O/M, whereas UO and UO_3 show a rather large sensitivity.

The O_2 partial pressures are not quoted because they are always at least one order of magnitude lower than the atomic oxygen pressures and, therefore, do not constitute an important contribution to the total pressure. However, the oxygen potential can be estimated easily from eq.(38) if so desired, for example for comparison with other evaluations.

In addition to the substoichiometric range, partial pressure tables for O/M = 2.01 and 2.08 are included. They are of interest for comparison with the Breitung and Reil /2/ data. These authors used samples with an original O/M of 2.01 (EEOSO4 and O5) and 2.08 (EEOSO6 and O7). The calculated ratio of the total pressures (O/M = 2.08 and 2.01) is about 1.5 at 2200 J/g , and 1.15 at 3000J/g. Contrary to this, the experimental data clearly do not show any significant dependence at high specific enthalpies. One could speculate that, at the lower end of the experimental data, EEOSO5 should be more reliable than O4. This could confirm the expected trend at least at low fuel enthalpies. On other hand, at high fuel enthalpies, the expected difference is small anyway. This is, however, only speculation. Clear statements are not possible because the differences under consideration are in the range of experimental uncertainties. Besides, the samples tend to become substoichiometric at high temperatures.

5.3 Critical Point Data

Many authors predicted critical point data of UO_2, either on the basis of empirical relationships, or using theoretical models. A survey of the then available predictions was given by Ohse et al. /32/ in 1979. The critical temperature values vary between the limits 6000 and almost 10000K, while the majority of extrapolations seems to be in the range 7000 to 8000K. The recent work by Mistura et al. /11/, using a pertubed hard core model, is also in this range.
The present extrapolation leads to a higher value of the critical temperature. The predicted data for stoichiometric UO_2 are: T_c = 10 600K, ρ_c = 1.56 g/cm^3, p_c = 158 Mpa. The critical compressibility is then Z_c = 0.310, which is a reasonable value. Note that the atomic oxygen partial pressure in equilibrium with critical UO_2 is 230 Mpa, which must be added to the critical pressure to obtain the total pressure. These data are consistent with the recent experimental data and are, therefore, the most reliable prediction at the present state of the art. The main reason why the critical temperature is so high is the lower vapour pressure curve, in comparison to the early ones by Menzies /1/, or the IAEA recommendation /36/. The lower vapour pressure corresponds to a lower vapour density, and therefore to a higher critical temperature, where liquid and vapour density are equal.

The critical temperature depends, of course, on O/M, so that one has a critical line for the urania phase. This dependence, which is shown in Fig.4, is, however rather weak. Qualitatively, it is obvious that the vapour density increases with increasing O/M, thus leading to a slightly lower critical temperature. For the discussions in the later sections, where the rather weak dependence on O/M is disregarded, a round-off value of 10600 K will be used for the critical temperature.

5.4 Additional Results

The specific heat, C_p, as obtained by the present evaluation for stoichiometric UO_2, is shown in Fig.5 as a function of temperature. The value at the melting point, 0.473 J/gK, is close to the value 0.485 J/gK, which was recommended both by Rand et al. /29/, and by Fink et al. /33/, Fig.5. At higher temperatures, C_p from the present evaluation increases somewhat, with a maximum value of about 0.510 J/gK. This is not in agreement with Breitung /2/, who chose to use a decreasing C_p. Experimental data are available only up to 3500K /34/. Therefore, one has to rely on extrapolation, and it is certainly reasonable to use a physical model for this purpose. The evaluated vapour pressure fits very well the experimental data, both p(T) and p(H). One expects that electronic contributions to the specific heat play a role in the liquid, as temperatures (~ 0.5 - 1.0 eV) are reached which are typical of cold plasma temperatures. Such electronic contributions are not modelled in the SST, but they are implicit in the vapour pressure experiments, which were used to fit the SST model parameters. Thus,it is not surprising that one sees a slight increase in the liquid enthalpy, above the linear extrapolation of the Rand recommendation.

There is an enormous increase in enthalpy, and thus in the specific heat of solid UO_2 above ~ 2500K, which was discussed extensively in the literature /13, 29, 30/. It is attributed either to the formation of Frenkel defects, or to electronic disorder, or most likely to both of them. It is not clear how these effects should be extrapolated into the liquid. It is, therefore, somewhat surprising that the present model, which obviously does not account for either of these effects, reproduces the experimental C_p so well.

This result can be examined by looking at the relation

$$C_p = C_v + \frac{T\alpha^2}{\rho\beta}$$

where the specific heats are in J/gK, α is the liquid volume expansion coefficient, and β the compressibility (cm^3/J). The SST gives the following data at the melting point:

$$C_v = 0.278\,(J/gK) \qquad \alpha = 1.033 \times 10^{-4}\,(K^{-1})$$

$$C_p = 0.473\,(J/gK) \qquad \beta = 1.93 \times 10^{-5}\,(cm^3/J)$$

$$\rho = 8.86\,(g/cm^3) \qquad T_m = 3120\ K$$

Thus, SST leads to the following explanation: C_v has a "normal" value, about 9R, which is to be expected for a 3-atomic molecule. However, the difference C_p-C_v is large due to the low compressibility β. It is not suggested that this is the correct physical explanation, especially as the only available experiment gave a larger compressibility /35/. However, it seems to be a useful working hypothesis, which produces the correct C_p value , and should therefore, be used until more about the physical reality becomes known.

5.5 Analytical Fits

For the practical use of the results in fast reactor accident analysis codes, analytic fits were produced, especially for the vapour pressure, the liquid enthalpy and the density.
While the original evaluation is available for different O/M values, the fits were produced only for the stoichiometric case. It is felt that this is accurate enough for accident analysis. The dependence of the vapour pressure on O/M is significant only in the lower (liquid) temperature range (~ 3120 - 4000K), where the pressure is low anyway. In this Section, some analytical fits for the saturated liquid properties will be quoted and discussed.

-Saturation pressure (of the U-bearing species)

$$^{10}\log p_s(\mathrm{Mpa}) = 39.187 + 0.1921 \times 10^{-3} T - 34715/T - 3.8571 \ln T$$

-Total pressure (including oxygen)

$$^{10}\log p_{tot}(\mathrm{Mpa}) = 47.287 + 0.3615 \times 10^{-3} T - 36269/T - 4.8665 \ln T$$

-Saturation temperature, liquid C_v, liquid dp/dT as a function of the saturated liquid density

a) $2.15144 < \rho < 8.86(\mathrm{g/cm^3})$, $T_m < T_s < 10367.25$ K

$$T_s = T_m + (8.86 - \rho)/0.916 \times 10^{-3} - 1.7(8.86 - \rho)^2$$

$$C_v = 0.27813 + 0.044561(8.86 - \rho) - 0.013082(8.86 - \rho)^2 + 9.277 \times 10^{-4}(8.86 - \rho)^3$$

b) $\rho_c < \rho < 2.15144$ $(\mathrm{g/cm^3})$, $10367.25 \text{ K} < T_s < T_c$

$$T_s = 10600 - 427.13(\rho - 1.56)^2 - 681.12(\rho - 1.56)^3$$

$$C_v = 0.2597 + 0.015894(\rho - 1.56) - 1.675 \times 10^{-3}(\rho - 1.56)^2$$

$\frac{dp}{dT}$ can the be obtained from the thermodynamic relation

$$T\left(\frac{\partial p}{\partial T}\right)_\rho - p_s = \rho^2\left(-\frac{dU_{sat}}{d\rho} + C_v\frac{dT_{sat}}{d\rho}\right)$$

In these equations, T_s is in K, ρ in g/cm^3, C_v in J/gK, dp/dT in Mpa/K. T_c and ρ_c refer to the critical point, T_m is the melting temperature. The $T_s(\rho)$ curve follows the Drotning data /6/ in the vicinity of the melting point.

- Internal energy of the saturated liquid U_s(in J/g)

  a) In the range $U_m \leq U_s \leq 4271.0$ (J/g) or $T_m \leq T_s \leq 9000K$, the reference relation gives T_s as a function of U_s

$$T_s(U_s) = T_m + 2.1129x - 1.457 \times 10^{-4}x^2 + 4.2737 \times 10^{-8}x^3$$

$$x = U - U_m$$

The enthalpy at the melting point is $U_m = 1398.6$ J/g. This relation cannot be inverted analytically. However, an approximate inversion is

$$U = 1398.6 + 0.47419y + 1.6387 \times 10^{-5}y^2 - 2.3762 \times 10^{-9}y^3)$$

$$y = T - T_m$$

For given temperature, this can be used to find an approximate value for U, which can then be improved by iterating on T versus U equation.

b) Internal energy above 9000K

In the vicinity of the critical temperature, $U_s(T_s)$ is approximated by the form

$$U_c - U_s = \left(\frac{T_c - T_s}{\text{const}}\right)^{1/2}$$

where the constant must be suitably chosen. However, this equation holds only in the immediate neighbourhood of T_c. Therefore, the range 9000K to T_c was again subdivided, and the following equations were obtained

$$T_s = 9000 + 2.3334(U_s - 4271) \qquad \left\{ \begin{array}{l} 4271 < U_s < 4920.48 \\ 9000 < T < 10515.5 \end{array} \right.$$

$$T_s = T_c - 0.0161125(4992.9 - U)^2 \qquad \left\{ \begin{array}{l} 4920.48 < U_s < 4992.9 \\ 10515.5 < T < 10600 \end{array} \right.$$

Note that U_c = 4992.9 J/g. The analytical fits for the different regions have the same derivatives at their respective boundaries.

6. Summary and Conclusions

It was the goal of the present evaluation of the UO_2 equation of state to obtain agreement with the recent vapour pressure experiments which were carried out either in the ACRR test reactor, or by the laser surface heating techniques.
This goal could be fully achieved. In addition, these results are consistent with the "international average" vapour pressure at 2150K recommended by Ackermann. In view of this consistency, we agree with the error estimate by Breitung on the key variable, the vapour pressure, who suggested an error band which has a width of a factor of two. This is certainly good enough for reactor applications. Contrary to many earlier evaluations, where only UO_2 is considered in the gas phase, the present equation of state includes the partial pressures of UO, UO_2, UO_3 and atomic oxygen. The O_2 pressure is lower than that of atomic oxygen, and need not be explicitly included in the evaluation. The partial pressures clearly have larger uncertainties than the total pressure. This holds also for the large extrapolation of the oxygen partial pressure up to the critical temperature.
This new vapour pressure curve is lower, and has a lower slope than the curve by Menzies, which was considered standard so far. Consequently, the predicted critical temperature is significantly higher than that suggested by Menzies.
At the present state of the art, it is recommended to use the new UO_2 equation of state also in the accident analysis for mixed-oxide fueled fast reactors. The experiments by Breitung and Reil /2/ have shown that the vapour pressure of the two materials agree within the experimental errors. Besides, experimental data are more scarce for PuO_2 than for UO_2, so that an evaluation for mixed oxide necessarily would introduce additional open parameters and therefore such an evaluation would not provide additional information.
On the other hand, there are some well-known minor differences between mixed oxide and UO_2, notably in the melting temperature and in the density. The UO_2 EOS can be easily modified for these differences. It is, therefore, not planned to carry out an additional EOS evaluation for mixed oxide.
Analytical fits for the important variables of the new EOS

were obtained, to facilitate implementation into accident analysis codes.

It is known from parametric studies that the energy produced during a power excursion of a hypothetical accident is rather insensitive to variations of the vapor pressure curve. Qualitatively it is clear that a lower vapor pressure curve must lead to a higher thermal energy in the molten fuel. On the other hand, the efficiency of the conversion of thermal to work energy goes down in this case. The two effects compensate in part, and it is to be expected that the work energy depends even more weekly on the vapor pressure curve. Estimates have shown that going from the older Menzies curve to the new evaluated data can lead to an increase or a decrease of the work energy, with the change being typically of the order of 10 % in cases of interest.

List of Symbols

Latin Symbols

a	parameter of the SST model
C_v, C_p	specific heat at constant volume/pressure
D(E)	density of electronic states of gases
E_s	binding energy of the UO_2 crystal
F	Helmholtz free energy per mol
FEF	free energy function
f_s, f_g	partition function per molecule of UO_2 (solid/gas)
f_i	partition function per molecule of UO_i
g_o	ground state multiplicity
GPF	grand partition function per mol
ΔG_f^o	standard free energy of formation
ΔH_{sub}	heat of sublimation
h	Planck's constant
H^o	standard molar enthalpy
J	thermodynamic potential related to GFP
k	Boltzmann's constant
N	Avogadro's number
N_o	number of oxygen atoms per mol of urania
N_b	number of excess oxygen atoms beyond stoichiometry
N_i	number of oxygen interstitials per mol
N_v	number of oxygen vacancies per mol
N_1, N_2, N_3	number of UO, UO_2, UO_3 molecules per mol of gas
p	pressure
Q	component of the gas partition function
q_i, q_v	functions to account for the vibrational modes associated with oxygen defects (interstitials/vacancies)
R	gas constant
S	molar entropy
T	absolute temperature
U	molar internal energy
V	molar volume
V_s	molar volume of solid UO_2 at the melting temperature

x	deviation of O/M from stoichiometry
y_1, y_2, y_3	fraction of UO, UO_2, UO_3 in the gas phase
Z	partition function per mol
Z_{def}	oxygen point defect partition function per mol
Z_{gm}	partition function of mixture of U-bearing gas components

Greek Symbols

α	coefficient of thermal expansion of liquid UO_2
β	isothermal compressibility of liquid UO_2
γ	parameter of the SST model
ε_i	energy to remove an oxygen interstitial atom from the lattice to infinity
ε_v	energy to remove an oxygen lattice atom to infinity
μ_o	chemical potential of atomic oxygen
ρ	liquid density
Θ_E	Einstein temperature of the UO_2 crystal
Θ_i	$= \varepsilon_i/R$
Θ_v	$= \varepsilon_v/R$ and vibrational frequency
$\omega(E)$	energy level density

Subscripts/Superscripts

c	critical point
g,gas	gas
i	interstitital atom
l,liq	liquid
m	melting point
s	saturation
v	vacancy
v	vapour
trans	translational contribution
rot	rotational contribution
vib	vibrational contribution
el	electronic contribution

References

/1/ Menzies D.C.,
The Equation of State of Uranium Dioxide at High Temperatures and Pressures
UKAEA-Report TRG 1119(D) (1966)

/2/ Breitung W., and Reil K.O.,
In-Pile Vapour Pressure Measurements on UO_2 and $(U,Pu)O_2$.
KfK-3939 (1985)

/3/ Bober M., Singer J. and Trapp H.,
Boiling Point Measurements on Liquid UO_2. BNES Conference on Science and Technology of Fast Reactor Safety, Guernsey, Channel Islands, 11-16. May 1986, BNES, 1986, Vol. 1, p. 507-512

/4/ Ohse R.W. et al.,
Equation of State of Uranium Dioxide
J. Nuclear Mater. 130, p. 165 (1985)

/5/ Limon R. et al.,
Equation of State of Non-Irradiated UO_2
Proceedings of the ANS/ENS Topical Meeting on Reactor Safety Aspects of Fuel Behaviour, Sun Valley, Idaho, Aug. 2-6, 1981, Vol. 2, p. 229-236

/6/ Drotning W.D.,
Thermal Expansion of Molten Uranium Dioxide
Eighth Symposium on Thermophysical Properties, Gaithersburg, June 1981 (NBS), CONF-810696-1

/7/ Christensen J.A.,
Thermal Expansion and Change in Volume of Uranium Dioxide on Melting
J.Am.Ceram. Soc 39, 81 (1963)
see also USAEC Report HW-75148

/8/ Ackermann R.J., Rauh E.G., Rand M.H.,
A Re-determination and Re-assessment of the Thermodynamics of Sublimation of Uranium Dioxide.
IAEA Symposium on Thermodynamics of Nuclear Materials, Jülich 29.1.-2.2.1979, CONF-790111-2

/9/ Gillan M.J.,
Derivation of an Equation of State for liquid UO_2 using the theory of significant structures
IAEA Conference on Thermodynamics of Nuclear Materials, Vienna, 21-25 Oct. 1974
Proc.: Vienna: IAEA, 1975, Vol. 1, p. 269-284

/10/ Fischer E.A., Kinsman P.R., Ohse R.H.,
Critical Assessment of Equation of State Data for UO_2
J. Nuclear Mater. 59, 125 (1976)

/11/ Mistura L., Magill J., Ohse R.W.,
A Perturbed Hard Core Equation of State for Oxide Nuclear Fuels
J. Nucl. Mater. 135, 95 (1985)

/12/ Green D.W., Leibowitz L.,
Vapour Pressures and Vapour Compositions in Equilibrium with hypostoichiometric uranium dioxide at high temperatures.
J. Nucl. Mater. 105, 184 (1982)
see also Report ANL-CEN-RSD-81-1

/13/ Long K.A. et al.,
Consistency of Measurements and Calculations of the Total Pressure over UO_2 at High Temperatures
High Temperatures - High Pressures 12, 515 (1980)

/14/ Fischer E.A.,
Recent Improvements of Fuel Equation of State and Their Impact on the analysis of Energetic Excursions
BNES Conference on Science and Technology of Fast Reactor Safety, Guernsey, Channel Islands, 11-16 Mai 1986, BNES, 1986, Vol. 1, p. 495-500

/15/ Becker R.,
Theorie der Wärme
Springer Verlag, 1964

/16/ Fowler R., Guggenheim E.A.,
Statistical Thermodynamics
Cambridge University Press, 1952

/17/ Eyring H. and Jhon M.S.,
Significant Liquid Structures
Wiley, New York, 1969

/18/ Thorn R.J. and Winslow G.H.,
Non-Stoichiometry in Uranium Dioxide
J. Chem. Phys. 44, 2632 (1966)

/19/ Blackburn P.E.,
Oxygen Pressures over Fast Breeder Reactor Fuel
J. Nucl. Mater. 46, 244 (1973)

/20/ Catlow C.R.A.,
Non-Stoichiometric Oxides
Editor: Sorensen O.T.
Academic Press 1981

/21/ Hyland G.J.,
Oxygen Potential Model for Stoichiometric and Non-Stoichiometric Uranium Dioxide
Report EUR 9410 EN (1984)

/22/ Hildebrand D.L., Gurvich L.V., Yungman V.S.,
The Chemical Thermodynamics of Actinide Elements, Part 13:
The Gaseous Actinide Ions
IAEA, Vienna 1985

/23/ Stull D.R., Sinke G.C.,
Thermodynamic Properties of the Elements
American Chemical Society, Washington 1956

/24/ National Bureau of Standards
JANAF Thermochemical Tables, 2nd Edition (1971)

/25/ Green D.W.,
Calculation of the Thermodynamic Properties of Fuel-Vapour Species from Spectroscopic Data
Report ANL-CEN-RSD-80-2 (1980)

/26/ Brewer L., Rosenblatt G.M.,
Dissociation Energies and Free Energy Functions of Gaseous Monoxides
in: Advances in High Temperature Chemistry, Vol. 2, p. 1-83
Editor: Eyring L.
Academic Press, New York 1969

/27/ Chasanov M.G. et al.,
Reactor Safety and Physical Property Studies Annual Report
July 1973 - June 1984
Report ANL-8120

/28/ Kerley G.I. and Burns J.,
An Invitation to Participate in the LASL EOS Library
LASL-79-62 (1979)

/29/ Rand M.H., Ackermann R.J., Gronvold F., Oetting F.L., Pattoret A.,
The Thermodynamic Properties of the Urania Phase
Rev. Internat. Hautes Temperatures et Refract. 15, 355 (1978)

/30/ Mac Innes D.A. and Catlow C.R.A.,
Specific Heat Anomaly in Crystalline UO_2
J. Nucl. Mater. 89, 354 (1980)

/31/ Reedy G.T., Chasanov M.G.,
Total Pressure of Uranium-Bearing Species over Molten Urania
J. Nucl. Mater. 42, 341 (1972)

/32/ Ohse R.W. et al.,
Present State of Vapour Pressure Measurements up to 5000K and Critical Point Data Prediction of Uranium Dioxide
J.Nucl.Mater. 80, 232(1979)

/33/ Fink J.K., Chasanov M.G., Leibowitz L.,
Properties for Reactor Safety Analysis
Report ANL-CEN-RSD-82-2

/34/ Leibowitz L., Chasanov M.G., Mishler L.W., Fischer D.F.,
Enthalpy of Liquid Uranium Dioxide to 3500K
J.Nucl.Mater. 39, 115(1971)

/35/ Slagle O.D. and Nelson R.P.,
Compressibility of Molten UO_2
J.Nucl.Mater. 40, 349(1971)

/36/ International Working Group on Fast Reactors
Specialist's Meeting on "Equation of State of Materials of Relevance to the Analysis of Hypothetical Fast Breeder Reactor Accidents",
AERE Harwell, June 1978
Report IWGFR/26

Appendix A

Equations Used to Calculate Internal Energy and Pressure, and their Derivatives

For the applications of the present model to fast reactor accident analysis, the internal energy U, the pressure p, and their derivatives with respect to T and V are needed.
The equations to calculate these quantities can be developed from the theory described in Section 3. However, the derivations are not straightforward; therefore, a list of the relevant equations will be given in this Appendix.

A1. Some Basic Relations

Some basic equations relating U and p to the thermodynamic potential J are:

$$J = U - TS - \mu_o x$$

$$dJ = - SdT - pdV - xd\mu_o$$

$$S = -\left(\frac{\partial J}{\partial T}\right)_{V,\mu_o} \qquad p = -\left(\frac{\partial J}{\partial V}\right)_{T,\mu_o} \qquad x = -\left(\frac{\partial J}{\partial \mu_o}\right)_{T,V}$$

$$U = J - T\left(\frac{\partial J}{\partial T}\right)_{V,\mu_o} - \mu_o\left(\frac{\partial J}{\partial \mu_o}\right)_{T,V}$$

$$\left(\frac{\partial U}{\partial V}\right)_{T,\mu_o} = - p + T\left(\frac{\partial p}{\partial T}\right)_{V,\mu_o} + \mu_o\left(\frac{\partial x}{\partial V}\right)_{T,\mu_o}$$

$$\left(\frac{\partial U}{\partial \mu_o}\right)_{T,V} = T\left(\frac{\partial x}{\partial T}\right)_{V,\mu_o} + \mu_o \left(\frac{\partial x}{\partial \mu_o}\right)_{T,V}$$

A2. The Derivatives at Constant x

The thermodynamic potential J is a function of T, V, μ_o.
Therefore, the state variables which are obtained as derivatives with respect to T or V refer to the case μ_o = const.
Of primary interest are, however, the derivatives at constant composition, i.e. for x = const. This difference appears in C_V, $\partial p/\partial T$, etc. Expressions for these quantities are given in this Section.
Starting from the equation

$$dU = \left[\left(\frac{\partial U}{\partial T}\right)_{V,\mu_o} + \left(\frac{\partial U}{\partial \mu_o}\right)_{T,V} \left(\frac{\partial \mu_o}{\partial T}\right)_{V,x}\right] dT + \left[\left(\frac{\partial U}{\partial V}\right)_{T,\mu_o} + \left(\frac{\partial U}{\partial \mu_o}\right)_{T,V} \left(\frac{\partial \mu_o}{\partial V}\right)_{T,x}\right] dV$$

one obtains

$$C_{V,x} = \left(\frac{\partial U}{\partial T}\right)_{V,x} = \left(\frac{\partial U}{\partial T}\right)_{V,\mu_o} - \left[T \frac{\left(\frac{\partial x}{\partial T}\right)_{V,\mu_o}}{\left(\frac{\partial x}{\partial \mu_o}\right)_{T,V}} + \mu_o\right] \left(\frac{\partial x}{\partial T}\right)_{V,\mu_o}$$

$$C_{p,x} = C_{V,x} - T \frac{\left(\frac{\partial p}{\partial T}\right)_{V,x}^2}{\left(\frac{\partial p}{\partial V}\right)_{T,x}} = C_{V,x} + \frac{TV\alpha_x^{\ 2}}{\beta_x}$$

where

$$\alpha_x = \frac{1}{V}\left(\frac{\partial V}{\partial T}\right)_{p,x} \qquad \beta_x = -\frac{1}{\left(\frac{\partial p}{\partial V}\right)_{T,x}}$$

$$\left(\frac{\partial p}{\partial T}\right)_{V,x} = \left(\frac{\partial p}{\partial T}\right)_{V,\mu_o} - \frac{\left(\frac{\partial x}{\partial T}\right)\left(\frac{\partial x}{\partial V}\right)}{\left(\frac{\partial x}{\partial \mu_o}\right)_{T,V}}$$

$$\left(\frac{\partial p}{\partial V}\right)_{T,x} = \left(\frac{\partial p}{\partial V}\right)_{T,\mu_o} - \frac{\left(\frac{\partial x}{\partial V}\right)^2_{T,\mu_o}}{\left(\frac{\partial x}{\partial \mu_o}\right)_{T,V}}$$

A3. Evaluation of the Derivatives of the Non-Stoichiometric Part of the Thermodynamic Potential J.

According to eq.(33), the non-stoichiometric part of J is defined as

$$J_{non-st} = -RT\Phi(T,V,\mu_o,x,\Theta_V,y_1) - \mu_o x$$

together with the conditions

$$\Phi_x + \frac{\mu_o}{kT} = 0, \quad \Phi_{\Theta_V} = 0, \quad \Phi_{y_1} = 0$$

where ϕ_x etc. denote partial derivatives.
It is essentially due to these additional conditions that the evaluation of the derivatives is not straightforward, as opposed to the stoichiometric part, where they can be obtained in a trivial way. Note that it follows from the above conditions that also the total derivatives of these equations with respect to T, V, or μ_o vanish.

For example

$$\frac{d}{dT}(\Phi_x + \frac{\mu_o}{RT}) = \Phi_{xT} + \Phi_{xx}\frac{\partial x}{\partial T} + \Phi_{x\Theta_V}\frac{\partial \Theta_V}{\partial T} + \Phi_{xy_1}\frac{\partial y_1}{\partial T} - \frac{\mu_o}{RT^2} = 0$$

In the following equations , terms which are zero due to the above conditions are already left out. The derivatives of J are then

$$\frac{dJ}{dT} = - R\Phi - RT\Phi_T$$

$$\frac{dJ}{dV} = - RT\Phi_V$$

$$\frac{dJ}{d\mu_o} = - x$$

$$\frac{d^2J}{dT^2} = - R(2\Phi_T + \Phi_x\frac{\partial x}{\partial T}) - RT(\Phi_{TT} + \Phi_{Tx}\frac{\partial x}{\partial T} + \Phi_{T\Theta_V}\frac{\partial \Theta_V}{\partial T} + \Phi_{Ty_1}\frac{\partial y_1}{\partial T})$$

$$\frac{d^2J}{dTdV} = - R\Phi_V - RT(\Phi_{TV} + \Phi_{Vx}\frac{\partial x}{\partial T} + \Phi_{V\Theta_V}\frac{\partial \Theta_V}{\partial T} + \Phi_{Vy_1}\frac{\partial y_1}{\partial T})$$

$$\frac{d^2J}{dV^2} = - RT \quad \Phi_{VV} + \Phi_{Vx}\frac{\partial x}{\partial V} + \Phi_{V\Theta_V}\frac{\partial \Theta_V}{\partial V} + \Phi_{Vy_1}\frac{\partial y_1}{\partial V}$$

$$\frac{d^2J}{d\mu_o{}^2} = -\frac{\partial x}{\partial \mu_o}$$

$$\frac{d^2J}{dTd\mu_o} = -\frac{\partial x}{\partial T}$$

$$\frac{d^2J}{dVd\mu_o} = -\frac{\partial x}{\partial V}$$

Derivatives of ϕ:

$$\Phi_T = \frac{V_s}{V}(\ln Z_{def})_T + \frac{V - V_s}{V}(\ln Z_{gm})_T$$

$$\Phi_V = \frac{V_s}{V^2}(\ln Z_{gm} - \ln Z_{def})$$

$$\Phi_x = \frac{V_s}{V}(\ln Z_{def})_x + \frac{V - V_s}{V}(\ln Z_{gm})_x$$

$$\Phi_{TT} = \frac{V_s}{V}(\ln Z_{def})_{TT} + \frac{V - V_s}{V}(\ln Z_{gm})_{TT}$$

$$\Phi_{TV} = \frac{V_s}{V^2}((\ln Z_{gm})_T - (\ln Z_{def})_T)$$

$$\Phi_{Tx} = \frac{V_s}{V}(\ln Z_{def})_{T,x} + \frac{V - V_s}{V}(\ln Z_{gm})_{T,x}$$

$$\Phi_{T\Theta_V} = \frac{V_s}{V} (\ln Z_{def})_{T\Theta_V}$$

$$\Phi_{Ty_1} = \frac{V - V_s}{V} (\ln Z_{gm})_{Ty_1}$$

$$\Phi_{VV} = - \frac{2V_s}{V^3} (\ln Z_{gm} - \ln Z_{def})$$

$$\Phi_{Vx} = \frac{V_s}{V^2} ((\ln Z_{gm})_x - (\ln Z_{def})_x)$$

$$\Phi_{V\Theta_V} = - \frac{V_s}{V^2} (\ln Z_{def})_{\Theta_V}$$

$$\Phi_{Vy_1} = \frac{V_s}{V^2} (\ln Z_{gm})_{y_1}$$

A4. Variation of x, θ_v, y_1 with temperature and volume

From the three conditions

$$\Phi_x + \frac{\mu_o}{RT} = 0$$

$$\frac{\Theta_V(x + 2\Theta_V)}{(1 - \Theta_V)(1 - x - 2\Theta_V)} = A$$

$$\frac{y_1(x + y_1)}{(1 - x - 2\, y_1)^2} = a$$

one obtains the derivatives of x etc. with temperature by some lengthy, but straightforward manipulations. The results are:

$$\frac{dx}{dT}\left[\frac{V_s}{V}\frac{1}{(1-\Theta_V)(1-x-2\Theta_V)\,u}+(1-\frac{V_s}{V})\frac{1}{(1-x-2y_1)\,v}\right]$$

$$= -\frac{1}{RT^2}\left(\frac{V_s}{V}\varepsilon_i+\mu_o\right)-\frac{V_s}{V}\frac{2(1-\Theta_V)\;dA/dT}{(x+2\Theta_V)\,u}$$

$$-\left(1-\frac{V_s}{V}\right)\frac{(1-x-2y_1)(1+x)da/dT}{(x+y_1)\,v}+\frac{V_s}{V}\frac{d}{dT}\ln q_i$$

$$+\left(1-\frac{V_s}{V}\right)\frac{d}{dT}\ln\frac{f_3}{f_2}$$

$$u\,\frac{d\Theta_V}{dT}=(1-\Theta_V)(1-x-2\Theta_V)\,\frac{dA}{dT}-(\Theta_V+A(1-\Theta_V))\,\frac{dx}{dT}$$

$$v\,\frac{dy_1}{dT}=(1-x-2y_1)^2\,\frac{da}{dT}-(y_1+2a(1-x-2y_1))\,\frac{dx}{dT}$$

u and v are given by

$$u = x + 4\Theta_V + A(3 - x - 4\Theta_V)$$

$$v = x + 2y_1 + 4a(1 - x - 2y_1)$$

In a similar way, the derivatives with the specific volume are obtained

$$\frac{dx}{dV}\left[-\frac{V_s}{V}\frac{x+2\Theta_V+A(1-x-2\Theta_V)}{(x+2\Theta_V)(1-x-2\Theta_V)\ u}+\frac{V-V_s}{V}\frac{1}{v}\right.$$

$$\left.\left(-\frac{x+y_1+2a(1-x-2y_1)}{x+y_1}-\frac{x}{1-x-2y_1}\right)\right]$$

$$=\frac{V_s}{V^2}\left[-\ln\frac{x+2\Theta_V}{1-x-2\Theta_V}+\ln q_i+\frac{\varepsilon_i}{kT}+\ln\frac{x+y_1}{1-x-2y_1}-\ln\frac{f_3}{f_2}\right]$$

$$u\,\frac{d\Theta_V}{dV}=-(\Theta_V+A(1-\Theta_V))\,\frac{dx}{dV}$$

$$v\,\frac{dy_1}{dV}=-(y_1+2a(1-x-2y_1))\,\frac{dx}{dV}$$

Concerning the derivatives with respect to μ_o, only the quantity $dx/d\mu_o$ is of interest.

$$\frac{dx}{d\mu_o}\left[\frac{V_s}{V}\frac{x+2\Theta_V+A(1-x-2\Theta_V)}{u}\left(\frac{1}{x+2\Theta_V}+\frac{1}{1-x-2\Theta_V}\right)\right.$$

$$\left.-\frac{V'-V_s}{V}\frac{1}{v}\left(\frac{x+y_1+2a(1-x-2y_1)}{x+y_1}+\frac{x}{1-x-2y_1}\right)\right]=-\frac{1}{RT}$$

A5. Explicit Expressions for U,p and Their Derivatives

The Non-Stoichiometric contribution to the internal energy, U_{nst}, is given by

$$\frac{U_{nst}}{RT^2} = \frac{V_s}{V}\left[2\Theta_V\left(\frac{\varepsilon_V}{RT^2} - \frac{q_V'}{q_V}\right) + (x + 2\Theta_V)\left(\frac{q_i'}{q_i} - \frac{\varepsilon_i}{RT^2}\right)\right]$$

$$+ \frac{V - V_s}{V}\left[y_1\left(\frac{f_1'}{f_1} - \frac{f_2'}{f_2}\right) + (x + y_1)\left(\frac{f_3'}{f_3} - \frac{f_2'}{f_2}\right)\right]$$

The primes in this equation denote temperature derivatives. Each term has a simple meaning: In the solidlike lattice, there is the energy of $2\Theta_V$ oxygen vacancies, and of $(x+2\Theta_V)$ interstitial atoms per mol. Similarly, the energy of the gas phase deviates from the stoichiometric value because the phase contains y_1 moles of UO, and $(x+y_1)$ moles for UO_3.

As far as the gas phase is concerned, the present model gives the specific volume, and the O/M ratio; however, it does not give directly the composition in terms of the fractions of UO, UO_2 and UO_3. However, this equation suggests the following interpretation: There are two kinds of oxygen vacancies in the liquid, with different energies of formation; one is included in the solidlike PF, the other one in the gas PF. In the gas phase, i.e. for $V = V_{gas}$, they manifest themselves through the presence of UO(g), instead of UO_2(g). Thus, the fraction of UO(g) in the vapour phase is given by

$$2\Theta_V \frac{V_s}{V} + y_1 \frac{V - V_s}{V}$$

Similarly, the fraction of $UO_3(g)$ is

$$(x + 2\Theta_V)\frac{V_s}{V} + (x + y_1)\frac{V - V_s}{V}$$

These expressions hold in the "real gas" case, where the first terms are not negligible. Far away from the critical temperature (in practice up to ~ 5000K), where V_g is much larger than V_s, and the gas behaves ideally, the fractions are those given by the gaslike partition function.

The derivative

$$\left(\frac{\partial U}{\partial T}\right)_{V,\mu_o} = C_{V,\mu_o}$$

can be obtained from the above equation by straight-forward differentiation. The derivatives $\partial U/\partial V$ and $\partial U/\partial \mu_o$ can be expressed according to the equations in Section A1.
The non-stoichiometric contribution to the pressure is given by the equation

$$p_{nst} = RT\frac{V_s}{V^2}(\ln Z_{gm} - \ln Z_{def})$$

The temperature derivative is

$$\left(\frac{\partial p_{nst}}{\partial T}\right)_{V,\mu_o} = \frac{p_{nst}}{T} + RT\frac{V_s}{V^2}\Big[(\ln Z_{gm})_T - (\ln Z_{def})_T$$

$$+ (\ln Z_{gm})_x \frac{dx}{dT} - (\ln Z_{def})_x \frac{dx}{dT}\Big]$$

The volume derivative is

$$\left(\frac{\partial p_{nst}}{\partial V}\right)_{T,\mu_o} = - RT \frac{2V_s}{V^3} (\ln Z_{gm} - \ln Z_{def})$$

$$+ RT \frac{V_s}{V^2} ((\ln Z_{gm})_x - (\ln Z_{def})_x) \frac{dx}{dV}$$

Appendix B

Equations for the Gas Partition Functions

To complete the documentation of this work, the equations used for the partition functions of the gaseous species are quoted in this Appendix. The Born-Oppenheimer approximation is used throughout, which allows to separate the PF for the different degrees of freedom as follows

$$f_{gas} = Q^{trans}\, Q^{rot}\, Q^{vib}\, Q^{el}$$

Furthermore, unharmonic effects are neglected. The different contributions are given by the equations

$$Q^{trans} = \frac{(2\pi mkT)^{3/2}\, eV}{h^3 N}$$

$$Q^{rot} = \frac{8\pi^2 IkT}{h^2 \sigma} \qquad (UO \text{ and } UO_2)$$

$$Q^{rot} = \left(\frac{8\pi^2 kT}{h^2}\right)^{3/2} \frac{\pi^{1/2}(I_A I_B I_C)^{1/2}}{\sigma} \qquad (UO_3)$$

$$Q^{vib} = \pi \frac{1}{1 - \exp(-\frac{hc\omega_i}{kT})}$$

Nomenclature:

m	molecular mass (g)
$I = \mu a^2$	moment of inertia (gcm^2)
μ	reduced mass (g)
a	atomic distance (cm)
$I_{A,B,C}$	directional moments of inertia of UO_3
ω_i	oscillator frequencies (cm^{-1})
σ	symmetry number
	(1 for heteronuclear, 2 for homonuclear molecule)
k	Boltzmann's constant
h	Planck's constant
c	velocity of light

The data used for the different molecules are given in Table I. The electronic partition function is approximated by an analytic function, assuming a linear increase in the level density with temperature

$$Q^{el} = g_0(1 + \int_{E_e}^{\infty}(D + D'E)e^{-E/RT}\,dE)$$

where D and D' characterize the level density, and g_o is the multiplicity of the ground state. This is an extension of the function used earlier /10/, where the level density was assumed constant.

Table I: Input Parameters for SST: Data for the Gaslike Partition Functions

	UO	UO_2	UO_3
Bond length (nm)	0.1764	0.179	
Moment of inertia	7.74×10^{-39} gcm^2	1.702×10^{-37} gcm^2	1.806×10^{-57} g$^{3/2}$cm^3
Vibrational frequencies (cm^{-1}) (degeneracy)	825(1)	765(1)	843.5(1)
			745.6(1)
		190(2)	852.6(1)
		776.1	180(1)
			150(1)
			130(1)
Rotational degeneracy, σ	1	2	1
Lumped constant K_i	1.889	2.071	3.252

Table II: Free Energy Function (Base 298K) of UO_2(gas)

T	FEF (J/mol K)			
	Atomic States Model (a)	Green (ANL)(b)	Eq.(43)	Eq.(44)
1800	341.9	329.0	328.6	328.6
2200	353.6	340.6	340.5	340.5
2600	363.9	350.7	351.0	351.0
3000	373.0	359.5	360.2	360.3
4000	391.8	377.8	379.3	379.7
5000	406.8	392.4	394.5	395.3
6000	419.1	404.6	408.1	409.3

a) Chasanov, Ref. / 27 /

b) Ref. / 25 /

Table III: Free Energy Function (Base 298K) of UO(gas)

T(k)	Atomic States Model (a)	Green (ANL) (b)	This evaluation
1800	288.9	279.5	289.3
2200	296.5	286.9	298.1
2600	303.3	293.3	305.7
3000	309.6	298.9	312.4
4000	323.0	310.6	326.1
5000	334.2	320.0	337.0
6000	343.7	327.9	345.9

(a) Ref. /27/

(b) Ref. /25/

Table IV: Free Energy Function (Base 298K) of UO_3(gas) (J/mol K)

T(k)	Atomic States Model (a)	Green (ANL) (b)	This evaluation
1800	385.8	382.8	398.9
2200	399.3	397.0	415.4
2600	411.0	409.3	428.8
3000	421.2	420.2	441.2
4000	442.5	443.0	466.9
5000	459.4	461.2	487.4
6000	473.5	476.5	504.4

(a) Ref. /27/

(b) Ref. /25/

Table V: Comparison of Evaluated Partial Pressures with the TU Experimental Data (Pressures in Mpa)

This evaluation

T(K)	p(UO)	p(UO_2)	p(UO_3)	Ratio Γ	Ratio Γ (ANL evaluation)
3120	1.63×10^{-5}	2.53×10^{-3}	1.70×10^{-3}	0.066	0.051
3500	2.64×10^{-4}	1.63×10^{-2}	1.26×10^{-2}	0.112	0.067
4000	4.11×10^{-3}	0.100	8.94×10^{-2}	0.191	0.089
4500	3.16×10^{-2}	0.375	0.375	0.290	0.109
5000	0.150	1.00	1.10	0.406	0.128

Experiments at the European Institute for Transuranium Elements (TU)

T(K)	p(UO)	p(UO_2)	p(UO_3)	Ratio Γ
3500	6.01×10^{-4}	1.2×10^{-2}	8.3×10^{-3}	0.186
4000	3.98×10^{-3}	7.2×10^{-2}	8.59×10^{-2}	0.257
4500	1.73×10^{-2}	0.286	0.536	0.336
5000	.0562	0.871	2.31	0.414

$$\text{Ratio } \Gamma = \left[\frac{p(UO)\,p(UO_3)}{p(UO_2)^2} \right]^{1/2}$$

Table VI: Electronic Partition Function Parameters in Eq.(40) for UO, UO_2, UO_3

	UO	UO_2	UO_3
g_o	3.0	3.0	3.0
D_1 (mol/J)	7.648×10^{-4}	3.167×10^{-4}	6.692×10^{-4}
D_1 (mol^2/J^2)	10.96×10^{-9}	4.54×10^{-9}	9.59×10^{-9}
E_1 (J/mol)	22593	22593	33472

Reaction enthalpy $UO + O = UO_2$, ΔH_1 =-756.0 kJ/mol

Reaction enthalpy $UO_2 + O = UO_3$, ΔH_3 = 512.1 kJ/mol

Table VII: Oxygen Potentials (kJ/mol) in Equilibrium with Urania Calculated from Different Oxygen Potential Models (T = 3150K)

O/M	1.90	1.96	2.00
Winslow (1978),/12/			-2.36
Winslow (1979), /12/	-456	-379	
Chapman, /12/	-592	-443	-344
Bober, /12/			-251
Green and Leibowitz	-395	-344	-231
Blackburn, /19/	-447	-395	-264
Long et al,, /13/			-262
Hyland, /21/			-259
This work	-433	-386	-271

Table VIII: Model Parameters

E_s (kJ/mol)	515.05
V_s (cm^3/mol)	27.9
n	7.0
a	0.00297
γ	-0.11264
ε_v(kJ/mol)	734.29
ε_i(kJ/mol)	393.09
Θ_E(K)	159.11

Table IX: Partial Pressures (MPa) over Liquid Urania. O/M = 1.90

T(K)	x_g	P_{UO}	P_{UO_2}	P_{UO_3}	P_{sat}	P_O	P_{tot}
3120.0	-0.093	3.2280E-04	2.3112E-03	7.1941E-05	2.7059E-03	3.9510E-06	2.7099E-03
3500.0	-0.073	2.4949E-03	1.5014E-02	1.1304E-03	1.8639E-02	7.9370E-05	1.8718E-02
4000.0	-0.020	1.9273E-02	9.3515E-02	1.6679E-02	1.2947E-01	1.6473E-03	1.3111E-01
4500.0	0.045	9.1510E-02	3.5584E-01	1.1671E-01	5.6406E-01	1.6381E-02	5.8044E-01
5000.0	0.095	3.1445E-01	9.6494E-01	4.8234E-01	1.7617E+00	9.6450E-02	1.8582E+00
5500.0	0.121	8.5755E-01	2.0613E+00	1.3751E+00	4.2940E+00	3.8955E-01	4.6835E+00
6000.0	0.123	1.9581E+00	3.7116E+00	3.0302E+00	8.6999E+00	1.2003E+00	9.9002E+00
6500.0	0.110	3.8863E+00	5.9032E+00	5.5793E+00	1.5369E+01	3.0390E+00	1.8408E+01
7000.0	0.088	6.8879E+00	8.5633E+00	9.0499E+00	2.4501E+01	6.6498E+00	3.1151E+01
7500.0	0.062	1.1145E+01	1.1594E+01	1.3397E+01	3.6136E+01	1.3015E+01	4.9151E+01
8000.0	0.035	1.6757E+01	1.4893E+01	1.8533E+01	5.0183E+01	2.3339E+01	7.3521E+01
8500.0	0.009	2.3744E+01	1.8368E+01	2.4352E+01	6.6464E+01	3.9008E+01	1.0547E+02
9000.0	-0.015	3.2054E+01	2.1942E+01	3.0748E+01	8.4744E+01	6.1542E+01	1.4629E+02
9500.0	-0.038	4.1617E+01	2.5557E+01	3.7599E+01	1.0477E+02	9.2525E+01	1.9730E+02
10000.0	-0.060	5.2359E+01	2.9161E+01	4.4757E+01	1.2628E+02	1.3349E+02	2.5977E+02

Table X : Partial Pressures (MPa) over Liquid Urania. O/M = 1.92

T(K)	x_g	P_{UO}	P_{UO_2}	P_{UO_3}	P_{sat}	P_O	P_{tot}
3120.0	-0.063	2.6294E-04	2.3584E-03	9.1964E-05	2.7133E-03	4.9498E-06	2.7182E-03
3500.0	-0.033	2.0513E-03	1.5306E-02	1.4289E-03	1.8786E-02	9.8415E-05	1.8884E-02
4000.0	0.034	1.6143E-02	9.5168E-02	2.0623E-02	1.3193E-01	2.0018E-03	1.3394E-01
4500.0	0.106	7.8705E-02	3.6130E-01	1.3990E-01	5.7990E-01	1.9340E-02	5.9924E-01
5000.0	0.154	2.7879E-01	9.7725E-01	5.5799E-01	1.8140E+00	1.1022E-01	1.9243E+00
5500.0	0.173	7.8130E-01	2.0832E+00	1.5416E+00	4.4062E+00	4.3241E-01	4.8386E+00
6000.0	0.168	1.8218E+00	3.7457E+00	3.3168E+00	8.8843E+00	1.3032E+00	1.0188E+01
6500.0	0.149	3.6700E+00	5.9508E+00	6.0038E+00	1.5625E+01	3.2482E+00	1.8873E+01
7000.0	0.123	6.5725E+00	8.6254E+00	9.6220E+00	2.4820E+01	7.0293E+00	3.1849E+01
7500.0	0.093	1.0714E+01	1.1673E+01	1.4126E+01	3.6513E+01	1.3651E+01	5.0164E+01
8000.0	0.064	1.6195E+01	1.4987E+01	1.9420E+01	5.0602E+01	2.4341E+01	7.4943E+01
8500.0	0.036	2.3028E+01	1.8477E+01	2.5407E+01	6.6911E+01	4.0515E+01	1.0743E+02
9000.0	0.009	3.1186E+01	2.2067E+01	3.1966E+01	8.5220E+01	6.3719E+01	1.4894E+02
9500.0	-0.015	4.0579E+01	2.5694E+01	3.8975E+01	1.0525E+02	9.5569E+01	2.0082E+02
10000.0	-0.039	5.1164E+01	2.9311E+01	4.6276E+01	1.2675E+02	1.3760E+02	2.6435E+02

Table XI: Partial Pressures (MPa) over Liquid Urania. O/M = 1.94

T(K)	x_g	P_{UO}	P_{UO_2}	P_{UO_3}	P_{sat}	P_O	P_{tot}
3120.0	-0.028	2.0179E-04	2.4055E-03	1.2467E-04	2.7319E-03	6.5789E-06	2.7385E-03
3500.0	0.016	1.5980E-03	1.5595E-02	1.9042E-03	1.9098E-02	1.2873E-04	1.9226E-02
4000.0	0.100	1.2958E-02	9.6754E-02	2.6556E-02	1.3627E-01	2.5353E-03	1.3880E-01
4500.0	0.175	6.5891E-02	3.6629E-01	1.7175E-01	6.0393E-01	2.3420E-02	6.2735E-01
5000.0	0.217	2.4370E-01	9.8813E-01	6.5263E-01	1.8845E+00	1.2753E-01	2.0120E+00
5500.0	0.226	7.0678E-01	2.1024E+00	1.7355E+00	4.5447E+00	4.8267E-01	5.0274E+00
6000.0	0.214	1.6887E+00	3.7753E+00	3.6352E+00	9.0992E+00	1.4186E+00	1.0518E+01
6500.0	0.189	3.4582E+00	5.9930E+00	6.4622E+00	1.5913E+01	3.4759E+00	1.9389E+01
7000.0	0.158	6.2637E+00	8.6823E+00	1.0230E+01	2.5176E+01	7.4352E+00	3.2611E+01
7500.0	0.125	1.0290E+01	1.1743E+01	1.4886E+01	3.6919E+01	1.4322E+01	5.1242E+01
8000.0	0.092	1.5639E+01	1.5073E+01	2.0340E+01	5.1052E+01	2.5391E+01	7.6443E+01
8500.0	0.062	2.2330E+01	1.8576E+01	2.6483E+01	6.7389E+01	4.2083E+01	1.0947E+02
9000.0	0.034	3.0328E+01	2.2179E+01	3.3204E+01	8.5710E+01	6.5975E+01	1.5169E+02
9500.0	0.008	3.9560E+01	2.5822E+01	4.0379E+01	1.0576E+02	9.8705E+01	2.0447E+02
10000.0	-0.017	4.9981E+01	2.9449E+01	4.7820E+01	1.2725E+02	1.4183E+02	2.6908E+02

Table XII: Partial Pressures (MPa) over Liquid Urania. O/M = 1.96

T(K)	x_g	P_{UO}	P_{UO_2}	P_{UO_3}	P_{sat}	P_O	P_{tot}
3120.0	0.017	1.3935E-04	2.4522E-03	1.8762E-04	2.7792E-03	9.7129E-06	2.7889E-03
3500.0	0.083	1.1345E-03	1.5876E-02	2.7796E-03	1.9790E-02	1.8461E-04	1.9974E-02
4000.0	0.184	9.7573E-03	9.8215E-02	3.6339E-02	1.4431E-01	3.4174E-03	1.4773E-01
4500.0	0.255	5.3442E-02	3.7053E-01	2.1670E-01	6.4068E-01	2.9253E-02	6.6993E-01
5000.0	0.284	2.0988E-01	9.9714E-01	7.7167E-01	1.9787E+00	1.4945E-01	2.1281E+00
5500.0	0.281	6.3508E-01	2.1183E+00	1.9610E+00	4.7144E+00	5.4157E-01	5.2560E+00
6000.0	0.260	1.5599E+00	3.8003E+00	3.9876E+00	9.3478E+00	1.5476E+00	1.0895E+01
6500.0	0.228	3.2523E+00	6.0297E+00	6.9558E+00	1.6238E+01	3.7235E+00	1.9961E+01
7000.0	0.192	5.9616E+00	8.7319E+00	1.0872E+01	2.5565E+01	7.8685E+00	3.3434E+01
7500.0	0.155	9.8739E+00	1.1807E+01	1.5681E+01	3.7361E+01	1.5031E+01	5.2393E+01
8000.0	0.120	1.5092E+01	1.5149E+01	2.1292E+01	5.1532E+01	2.6491E+01	7.8023E+01
8500.0	0.088	2.1639E+01	1.8666E+01	2.7595E+01	6.7900E+01	4.3717E+01	1.1162E+02
9000.0	0.058	2.9475E+01	2.2283E+01	3.4486E+01	8.6243E+01	6.8314E+01	1.5456E+02
9500.0	0.031	3.8546E+01	2.5938E+01	4.1814E+01	1.0630E+02	1.0195E+02	2.0825E+02
10000.0	0.005	4.8783E+01	2.9578E+01	4.9424E+01	1.2778E+02	1.4618E+02	2.7397E+02

Table XIII: Partial Pressures (MPa) over Liquid Urania. O/M = 1.98

T(K)	x_g	P_{UO}	P_{UO_2}	P_{UO_3}	P_{sat}	P_O	P_{tot}
3120.0	0.097	7.5358E-05	2.4976E-03	3.5990E-04	2.9329E-03	1.8292E-05	2.9512E-03
3500.0	0.195	6.6639E-04	1.6131E-02	4.8858E-03	2.1684E-02	3.1935E-04	2.2003E-02
4000.0	0.297	6.6756E-03	9.9382E-02	5.4384E-02	1.6044E-01	5.0522E-03	1.6549E-01
4500.0	0.345	4.1744E-02	3.7367E-01	2.8214E-01	6.9756E-01	3.7773E-02	7.3533E-01
5000.0	0.353	1.7832E-01	1.0037E+00	9.2029E-01	2.1023E+00	1.7710E-01	2.2794E+00
5500.0	0.336	5.6732E-01	2.1304E+00	2.2204E+00	4.9181E+00	6.1005E-01	5.5282E+00
6000.0	0.305	1.4365E+00	3.8199E+00	4.3749E+00	9.6313E+00	1.6911E+00	1.1322E+01
6500.0	0.267	3.0528E+00	6.0602E+00	7.4854E+00	1.6598E+01	3.9918E+00	2.0590E+01
7000.0	0.226	5.6666E+00	8.7740E+00	1.1548E+01	2.5989E+01	8.3307E+00	3.4320E+01
7500.0	0.186	9.4650E+00	1.1862E+01	1.6511E+01	3.7838E+01	1.5779E+01	5.3617E+01
8000.0	0.148	1.4554E+01	1.5218E+01	2.2279E+01	5.2051E+01	2.7642E+01	7.9693E+01
8500.0	0.114	2.0956E+01	1.8747E+01	2.8743E+01	6.8446E+01	4.5418E+01	1.1386E+02
9000.0	0.082	2.8638E+01	2.2375E+01	3.5788E+01	8.6801E+01	7.0743E+01	1.5754E+02
9500.0	0.054	3.7526E+01	2.6039E+01	4.3286E+01	1.0685E+02	1.0531E+02	2.1216E+02
10000.0	0.026	4.7639E+01	2.9692E+01	5.1001E+01	1.2833E+02	1.5068E+02	2.7901E+02

Table XIV: Partial Pressures (MPa) over Liquid Urania. O/M = 1.99

T(K)	x_g	P_{UO}	P_{UO_2}	P_{UO_3}	P_{sat}	P_O	P_{tot}
3120.0	0.185	4.3316E-05	2.5182E-03	6.3649E-04	3.1980E-03	3.2078E-05	3.2301E-03
3500.0	0.289	4.4467E-04	1.6231E-02	7.4124E-03	2.4088E-02	4.8148E-04	2.4569E-02
4000.0	0.367	5.2907E-03	9.9759E-02	6.9140E-02	1.7419E-01	6.3978E-03	1.8059E-01
4500.0	0.392	3.6452E-02	3.7467E-01	3.2483E-01	7.3596E-01	4.3375E-02	7.7934E-01
5000.0	0.387	1.6369E-01	1.0059E+00	1.0070E+00	2.1766E+00	1.9337E-01	2.3699E+00
5500.0	0.363	5.3522E-01	2.1349E+00	2.3634E+00	5.0335E+00	6.4823E-01	5.6818E+00
6000.0	0.327	1.3771E+00	3.8274E+00	4.5815E+00	9.7859E+00	1.7686E+00	1.1555E+01
6500.0	0.286	2.9559E+00	6.0729E+00	7.7634E+00	1.6792E+01	4.1340E+00	2.0926E+01
7000.0	0.243	5.5220E+00	8.7924E+00	1.1901E+01	2.6215E+01	8.5728E+00	3.4788E+01
7500.0	0.202	9.2641E+00	1.1886E+01	1.6939E+01	3.8090E+01	1.6168E+01	5.4258E+01
8000.0	0.162	1.4288E+01	1.5248E+01	2.2784E+01	5.2319E+01	2.8237E+01	8.0557E+01
8500.0	0.127	2.0619E+01	1.8783E+01	2.9325E+01	6.8727E+01	4.6294E+01	1.1502E+02
9000.0	0.094	2.8225E+01	2.2417E+01	3.6450E+01	8.7092E+01	7.1988E+01	1.5908E+02
9500.0	0.065	3.7040E+01	2.6088E+01	4.4022E+01	1.0715E+02	1.0702E+02	2.1417E+02
10000.0	0.037	4.7056E+01	2.9744E+01	5.1814E+01	1.2861E+02	1.5298E+02	2.8159E+02

Table XV: Partial Pressures (MPa) over Liquid Urania. O/M = 2.00

T(K)	x_g	P_{UO}	P_{UO_2}	P_{UO_3}	P_{sat}	P_O	P_{tot}
3120.0	0.397	1.6318E-05	2.5296E-03	1.7049E-03	4.2509E-03	8.5475E-05	4.3364E-03
3500.0	0.423	2.6333E-04	1.6274E-02	1.2584E-02	2.9122E-02	8.1515E-04	2.9937E-02
4000.0	0.441	4.1028E-03	9.9920E-02	8.9447E-02	1.9347E-01	8.2613E-03	2.0173E-01
4500.0	0.439	3.1658E-02	3.7519E-01	3.7507E-01	7.8192E-01	5.0019E-02	8.3194E-01
5000.0	0.421	1.5023E-01	1.0074E+00	1.1003E+00	2.2580E+00	2.1143E-01	2.4694E+00
5500.0	0.390	5.0436E-01	2.1384E+00	2.5161E+00	5.1588E+00	6.8909E-01	5.8479E+00
6000.0	0.350	1.3192E+00	3.8334E+00	4.7976E+00	9.9502E+00	1.8502E+00	1.1800E+01
6500.0	0.305	2.8606E+00	6.0840E+00	8.0513E+00	1.6996E+01	4.2823E+00	2.1278E+01
7000.0	0.260	5.3792E+00	8.8087E+00	1.2262E+01	2.6450E+01	8.8235E+00	3.5273E+01
7500.0	0.217	9.0648E+00	1.1909E+01	1.7377E+01	3.8351E+01	1.6568E+01	5.4919E+01
8000.0	0.176	1.4022E+01	1.5276E+01	2.3304E+01	5.2602E+01	2.8849E+01	8.1451E+01
8500.0	0.140	2.0280E+01	1.8819E+01	2.9929E+01	6.9028E+01	4.7193E+01	1.1622E+02
9000.0	0.107	2.7809E+01	2.2458E+01	3.7127E+01	8.7394E+01	7.3263E+01	1.6066E+02
9500.0	0.077	3.6540E+01	2.6133E+01	4.4776E+01	1.0745E+02	1.0878E+02	2.1623E+02
10000.0	0.048	4.6474E+01	2.9798E+01	5.2653E+01	1.2892E+02	1.5532E+02	2.8424E+02

Table XVI: Partial Pressures (MPa) over Liquid Urania. O/M = 2.01

T(K)	x_g	P_{UO}	P_{UO_2}	P_{UO_3}	P_{sat}	P_O	P_{tot}
3120.0	0.640	6.1337E-06	2.5184E-03	4.5016E-03	7.0261E-03	2.2624E-04	7.2523E-03
3500.0	0.560	1.5562E-04	1.6236E-02	2.1194E-02	3.7586E-02	1.3762E-03	3.8962E-02
4000.0	0.514	3.1782E-03	9.9836E-02	1.1528E-01	2.1829E-01	1.0654E-02	2.2895E-01
4500.0	0.485	2.7477E-02	3.7521E-01	4.3218E-01	8.3487E-01	5.7641E-02	8.9251E-01
5000.0	0.454	1.3759E-01	1.0080E+00	1.2030E+00	2.3486E+00	2.3105E-01	2.5796E+00
5500.0	0.416	4.7524E-01	2.1406E+00	2.6760E+00	5.2918E+00	7.3239E-01	6.0242E+00
6000.0	0.371	1.2635E+00	3.8377E+00	5.0204E+00	1.0122E+01	1.9351E+00	1.2057E+01
6500.0	0.324	2.7681E+00	6.0935E+00	8.3462E+00	1.7208E+01	4.4350E+00	2.1643E+01
7000.0	0.277	5.2401E+00	8.8235E+00	1.2630E+01	2.6693E+01	9.0800E+00	3.5773E+01
7500.0	0.232	8.8692E+00	1.1929E+01	1.7821E+01	3.8619E+01	1.6977E+01	5.5596E+01
8000.0	0.190	1.3764E+01	1.5303E+01	2.3823E+01	5.2890E+01	2.9469E+01	8.2359E+01
8500.0	0.153	1.9951E+01	1.8851E+01	3.0525E+01	6.9326E+01	4.8102E+01	1.1743E+02
9000.0	0.119	2.7402E+01	2.2494E+01	3.7802E+01	8.7698E+01	7.4554E+01	1.6225E+02
9500.0	0.088	3.6057E+01	2.6176E+01	4.5525E+01	1.0776E+02	1.1055E+02	2.1830E+02
10000.0	0.059	4.5888E+01	2.9845E+01	5.3495E+01	1.2923E+02	1.5766E+02	2.8689E+02

Table XVII: Partial Pressures (MPa) over Liquid Urania. O/M = 2.08

T(K)	x_g	P_{UO}	P_{UO_2}	P_{UO_3}	P_{sat}	P_O	P_{tot}
3120.0	0.921	8.7793E-07	2.3587E-03	2.7552E-02	2.9911E-02	1.4800E-03	3.1391E-02
3500.0	0.866	2.9689E-05	1.5331E-02	9.9076E-02	1.1444E-01	6.8142E-03	1.2125E-01
4000.0	0.784	9.4732E-04	9.5657E-02	3.5586E-01	4.5246E-01	3.4477E-02	4.8694E-01
4500.0	0.708	1.1800E-02	3.6497E-01	9.5212E-01	1.3289E+00	1.3068E-01	1.4596E+00
5000.0	0.637	7.6740E-02	9.9278E-01	2.0921E+00	3.1616E+00	4.0882E-01	3.5705E+00
5500.0	0.572	3.1440E-01	2.1268E+00	3.9931E+00	6.4343E+00	1.1046E+00	7.5390E+00
6000.0	0.508	9.2802E-01	3.8242E+00	6.7871E+00	1.1539E+01	2.6380E+00	1.4177E+01
6500.0	0.447	2.1842E+00	6.1127E+00	1.0644E+01	1.8941E+01	5.6636E+00	2.4604E+01
7000.0	0.388	4.3321E+00	8.8724E+00	1.5446E+01	2.8651E+01	1.1103E+01	3.9754E+01
7500.0	0.334	7.5717E+00	1.2012E+01	2.1168E+01	4.0752E+01	2.0148E+01	6.0900E+01
8000.0	0.285	1.2017E+01	1.5422E+01	2.7714E+01	5.5153E+01	3.4243E+01	8.9396E+01
8500.0	0.241	1.7705E+01	1.9005E+01	3.4962E+01	7.1672E+01	5.5034E+01	1.2671E+02
9000.0	0.201	2.4628E+01	2.2681E+01	4.2762E+01	9.0071E+01	8.4307E+01	1.7438E+02
9500.0	0.166	3.2743E+01	2.6399E+01	5.0992E+01	1.1013E+02	1.2386E+02	2.3400E+02
10000.0	0.133	4.2010E+01	3.0106E+01	5.9460E+01	1.3158E+02	1.7530E+02	3.0688E+02

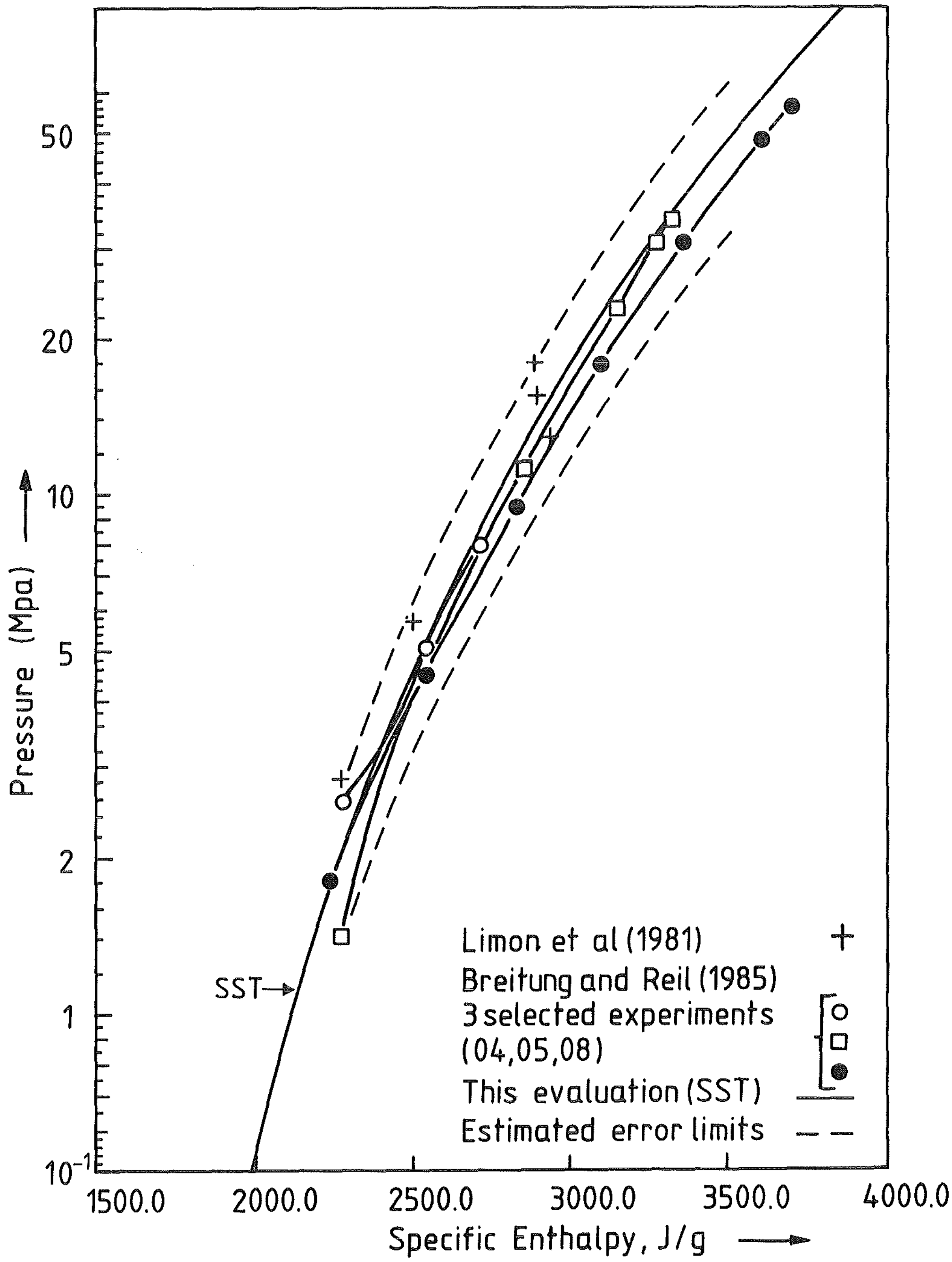

Fig. 1: Total Pressure over Liquid UO_2 Versus Specific Enthalpy

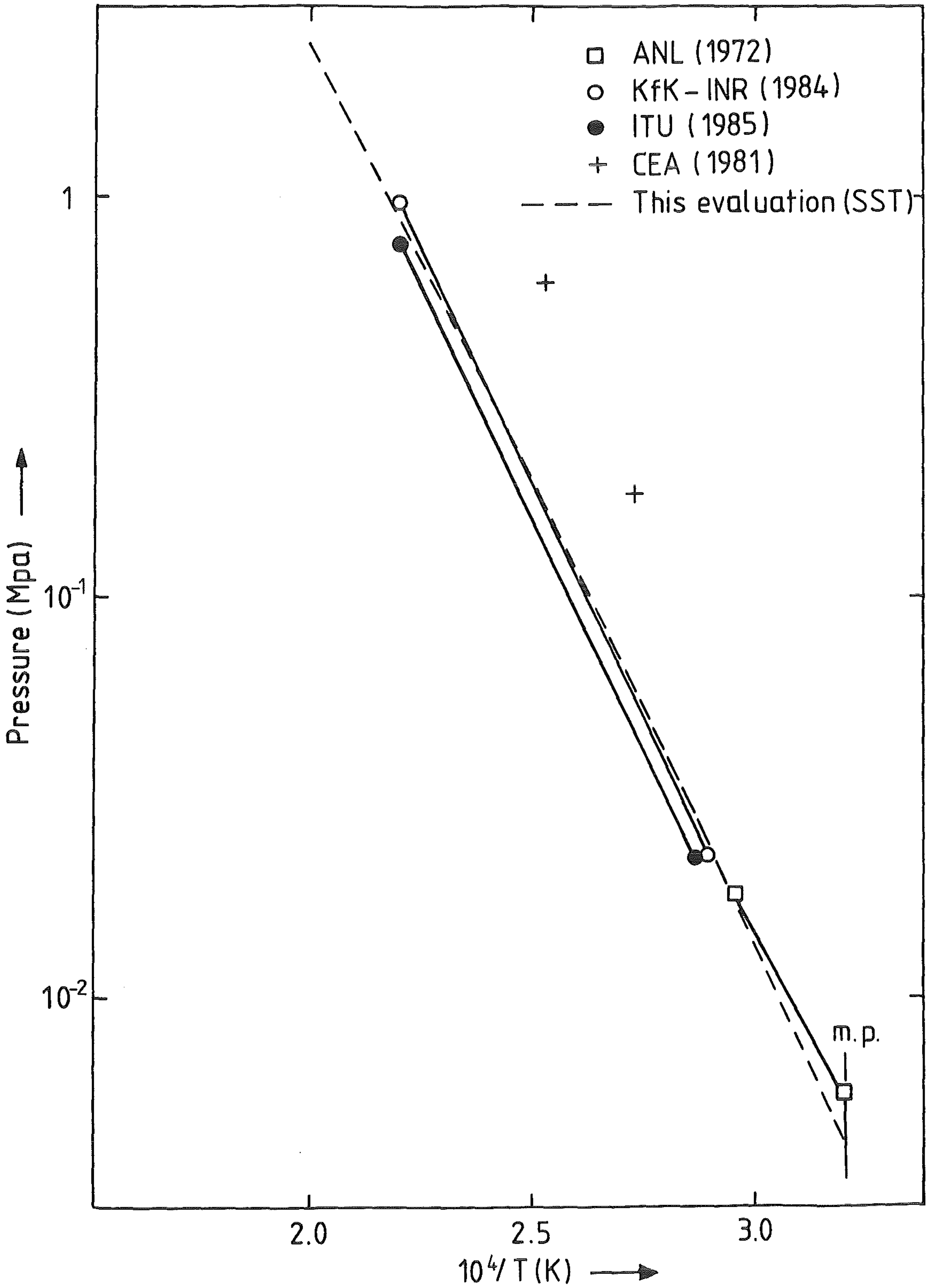

Fig. 2: Total Pressure over Liquid UO_2 Versus Inverse Temperature (m.p.= melting point)

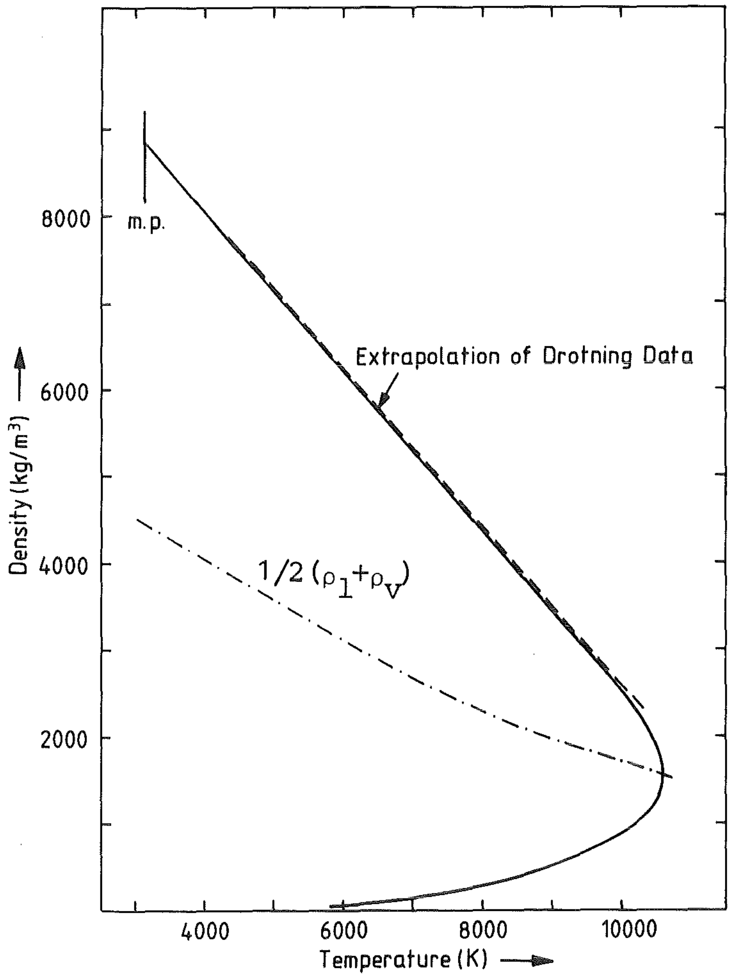

Fig.3: Density of the Saturated Liquid and Vapour
(m.p. = melting point)

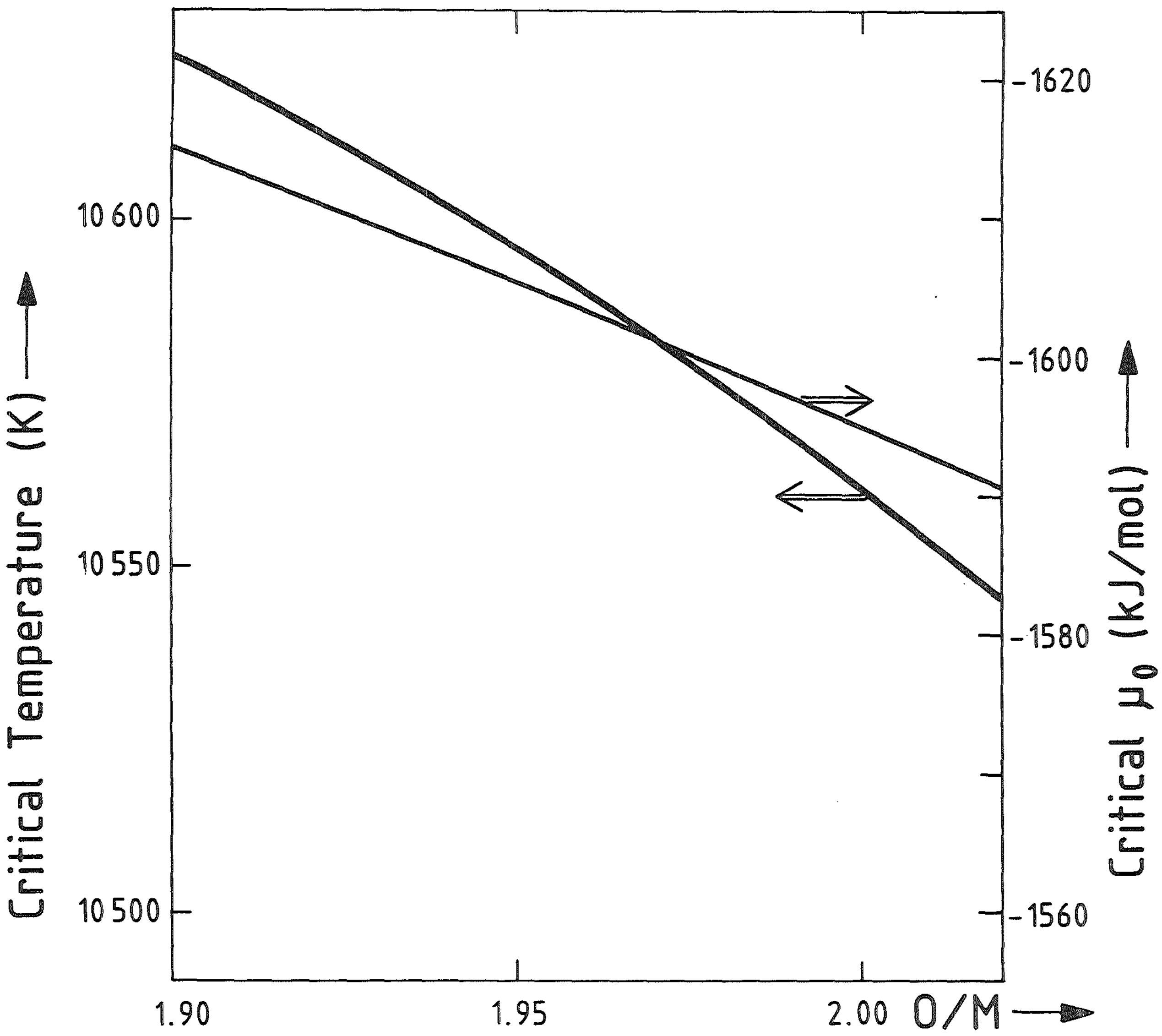

Fig. 4 Critical Line of Urania

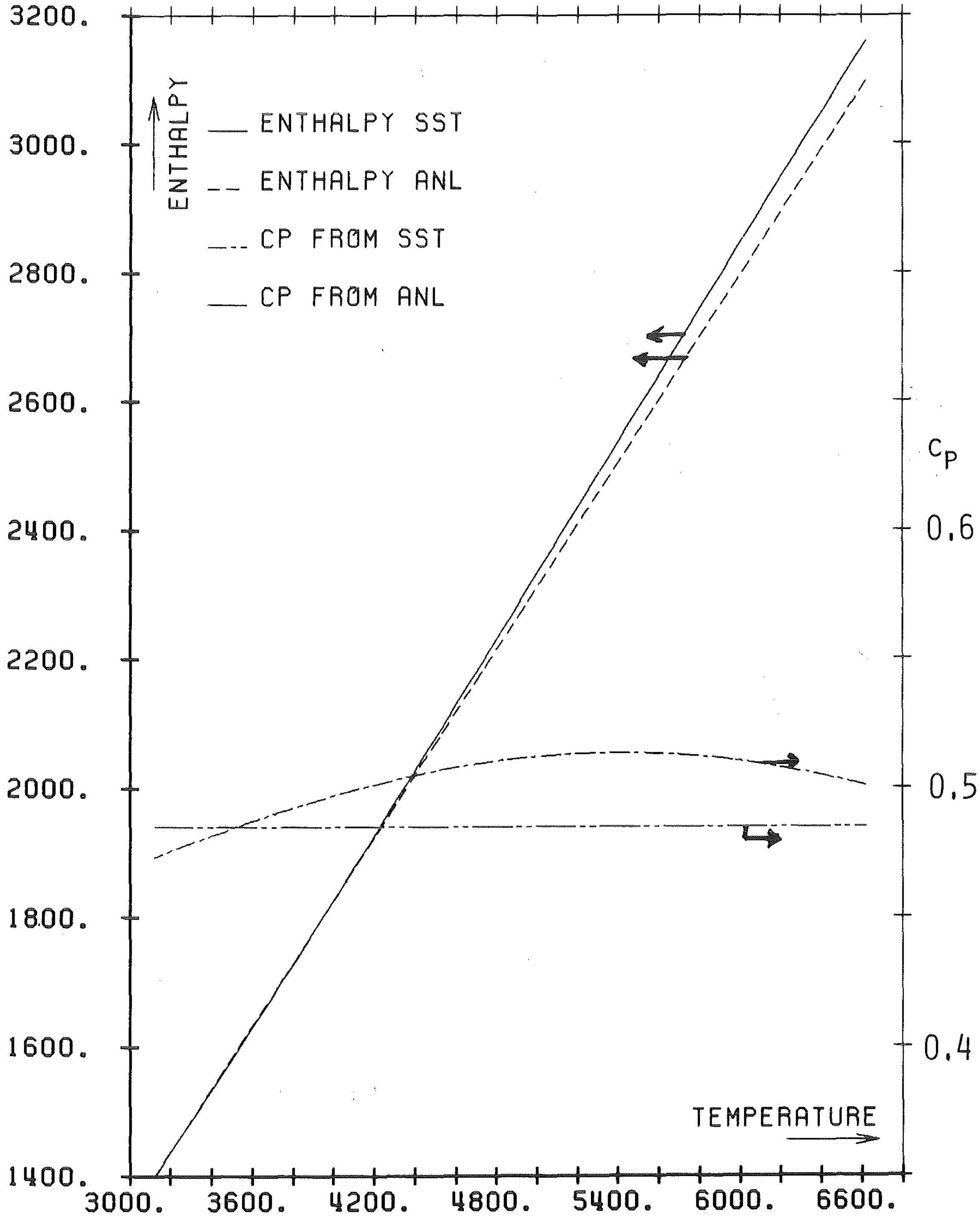

FIG. 5 ENTHALPY (J/G) AND CP (J/G-K) VS TEMP (K)